

1 **Selection and local adaptation in capuchin monkeys revealed through fluorescence-**  
2 **activated cell sorting of feces (fecalFACS)**

3

4 Joseph D. Orkin<sup>1,2\*</sup>, Michael J. Montague<sup>3</sup>, Daniela Tejada-Martinez<sup>4,5</sup>, Marc de Manuel<sup>2</sup>, Javier  
5 del Campo<sup>6</sup>, Anthony Di Fiore<sup>7,8</sup>, Claudia Fontserè<sup>2</sup>, Jason A. Hodgson<sup>9,10</sup>, Mareike C. Janiak<sup>1,11</sup>,  
6 Lukas F.K. Kuderna<sup>2</sup>, Esther Lizano<sup>2,18</sup>, Yoshihito Niimura<sup>12</sup>, George H. Perry<sup>9,13</sup>, Jia Tang<sup>1</sup>,  
7 Wesley C. Warren<sup>14</sup>, João Pedro de Magalhães<sup>5</sup>, Shoji Kawamura<sup>15</sup>, Tomàs Marquès-  
8 Bonet<sup>2,16,17,18</sup>, Roman Krawetz<sup>19</sup>, Amanda D. Melin<sup>1,11,20\*</sup>

9

- 10 1 Department of Anthropology and Archaeology, University of Calgary, Calgary, Canada  
11 2 Institut de Biologia Evolutiva, Universitat Pompeu Fabra-CSIC, Barcelona, Spain  
12 3 Department of Neuroscience, Perelman School of Medicine, University of Pennsylvania,  
13 Philadelphia, PA 19146  
14 4 Doctorado en Ciencias mención Ecología y Evolución, Instituto de Ciencias Ambientales  
15 y Evolutivas, Facultad de Ciencias, Universidad Austral de Chile, Valdivia, Chile  
16 5 Integrative Genomics of Ageing Group, Institute of Ageing and Chronic Disease,  
17 University of Liverpool, Liverpool L7 8TX, UK  
18 6 Department of Marine Biology and Ecology, Rosenstiel School of Marine and  
19 Atmospheric Science, University of Miami, Miami, FL, USA  
20 7 Department of Anthropology and Primate Molecular Ecology and Evolution Laboratory,  
21 University of Texas at Austin  
22 8 College of Biological and Environmental Sciences, Universidad San Francisco de Quito,  
23 Cumbayá, Ecuador  
24 9 Department of Anthropology, The Pennsylvania State University, State College, PA,  
25 USA  
26 10 Department of Zoology, University of Cambridge, Cambridge, UK  
27 11 Alberta Children's Hospital Research Institute, Calgary, AB, Canada  
28 12 Department of Applied Biological Chemistry, Graduate School of Agricultural and Life  
29 Sciences, The University of Tokyo, 1-1-1 Yayoi, Bunkyo-ku, Tokyo 113-8657, Japan  
30 13 Department of Biology, Huck Institute of Life Sciences, The Pennsylvania State  
31 University, State College, PA, USA  
32 14 Division of Animal Sciences, School of Medicine, University of Missouri, Columbia, MO,  
33 65211, USA  
34 15 Department of Integrated Biosciences, Graduate School of Frontier Sciences, The  
35 University of Tokyo, 5-1-5 Kashiwanoha, Kashiwa, Chiba 277-8562, Japan  
36 16 Catalan Institution of Research and Advanced Studies (ICREA), Passeig de Lluís  
37 Companys, 23, 08010, Barcelona, Spain  
38 17 CNAG-CRG, Centre for Genomic Regulation (CRG), Barcelona Institute of Science and  
39 Technology (BIST), Baldori i Reixac 4, 08028 Barcelona, Spain  
40 18 Institut Català de Paleontologia Miquel Crusafont, Universitat Autònoma de Barcelona,  
41 Edifici ICTA-ICP, c/ Columnes s/n, 08193 Cerdanyola del Vallès, Barcelona, Spain  
42 19 Department of Cell Biology and Anatomy, Cumming School of Medicine, University of  
43 Calgary, Calgary, Alberta, Canada

44 20 Department of Medical Genetics, Cumming School of Medicine, University of Calgary,  
45 Calgary, AB, Canada

46

47 \* Corresponding authors

48

49 **ABSTRACT**

50 Background: Capuchins have the largest relative brain size of any monkey and a  
51 remarkable lifespan of 55 years, despite their small body size. Distributed widely across Central  
52 and South America, they are inventive and extractive foragers, known for their sensorimotor  
53 intelligence, dietary diversity, and ecological flexibility. Despite decades of research into their  
54 ecology and life history, little is known about the genomics of this radiation.

55 Results: We assemble a *de novo* reference genome for *Cebus imitator*, and provide the  
56 first genome annotation of a capuchin monkey. We identified 20,740 and 9,556 for protein-  
57 coding and non-coding genes, and recovered 23,402 orthologous groups. Through a  
58 comparative genomics approach across a diversity of mammals, we identified genes under  
59 positive selection associated with longevity and brain development, which are of particular  
60 relevance to capuchin and primate comparative biology. Additionally, we compared populations  
61 in distinct habitats, facilitated by our novel method for minimally-biased, whole-genome  
62 sequencing from fecal DNA using fluorescence activated cell sorting (FACS). By analyzing 23  
63 capuchin genomes from tropical dry forest and rainforest, we identified population divergence in  
64 genes involved in water balance, kidney function, and metabolism, consistent with local  
65 adaptation to resource seasonality.

66 Conclusions: Our comparative study of capuchin genomics provides new insights into  
67 the molecular basis of brain evolution and longevity. These data also improve our understanding  
68 of processes of local adaptation to diverse and physiologically challenging environments.  
69 Additionally, we provide a technological advancement in use of non-invasive genomics to study  
70 free-ranging mammals through FACS.

71

72 **KEYWORDS**

73

74 Brain size, longevity, intelligence, seasonality, dry forest, non-invasive genomics, flow

75 cytometry, platyrrhine

76

77 **BACKGROUND**

78

79 Large brains, long lifespans, extended juvenescence, tool use, and problem solving are  
80 hallmark characteristics of the great apes, and are of enduring interest in studies of human  
81 evolution [1–6]. Similar suites of traits have arisen in other lineages, including some cetaceans,  
82 corvids and, independently, in another radiation of primates, the capuchin monkeys. Like great  
83 apes, they have diverse diets, consume and seek out high-energy resources, and engage in  
84 complex extractive foraging techniques [7,8] to consume difficult-to-access invertebrates and  
85 nuts [8]. Their propensity for tool use and their ecological flexibility may have contributed to their  
86 convergence with the great apes [9] offering opportunities for understanding their evolution via  
87 comparative methods [10–12].

88 Capuchins also offer excellent opportunities to study local adaptation to diverse habitats.  
89 While little is known about the migration, history, and population dynamics of this species, they  
90 presently range from Panama to northern Honduras [13–15], where they occupy a wide diversity  
91 of habitats, including rainforests and, in the northern extent of their range, tropical dry forests.  
92 Particular challenges of the tropical dry forest are staying hydrated during the seasonally  
93 prominent droughts, high temperatures in the absence of foliage, and coping metabolically with  
94 periods of fruit dearth (Figure 1). The sensory challenges of food search in dry versus humid  
95 biomes are also distinct. For example, odor detection and propagation is affected by  
96 temperature and humidity [16,17], and color vision is hypothesized to be adaptive in the search  
97 for ripe fruits and young reddish leaves against a background of thick, mature foliage [18], which

98 is absent for long stretches in dry deciduous forests. The behavioral plasticity of capuchins is  
99 widely acknowledged as a source of their ability to adapt to these dramatically different habitats  
100 [19–22]. However, physiological processes including water balance and metabolic adaptations  
101 to low caloric intake, and sensory adaptations to food search, are also anticipated to be targets  
102 of natural selection, as seen in other mammals [23–26].

103 Comparative genomics offers a unique opportunity to examine the molecular  
104 underpinnings of traits relevant to the evolution of humans and other great apes. Furthermore,  
105 the ecological flexibility of white-faced capuchins allows us to assess the influence of divergent  
106 and changing habitats on the process of adaptive evolution in these primates. In order to  
107 address the genetic underpinnings of capuchin adaptive evolution, we assembled the first  
108 reference genome of *Cebus imitator*. Additionally, to better understand the local adaptation of  
109 capuchins, we conducted high-coverage re-sequencing (10X - 47X) of 10 individuals from  
110 populations inhabiting distinct environments--one in a lowland evergreen rainforest (n=4), and  
111 another from a lowland tropical dry forest (n=6). Importantly, to facilitate the population-wide  
112 analyses without the need for potentially harmful invasive sampling of wild primates, we  
113 sequenced an additional 13 individuals at low coverage using a novel method for minimally-  
114 biased, whole-genome sequencing from fecal DNA using fluorescence-activated cell sorting  
115 (fecalFACS) that we developed (Figure 2). In our positive selection analyses, we focus on  
116 genes that may underlie sensation, cognition, and lifespan due to their relevance to capuchin-  
117 specific biology and adaptation. In our population comparison we predict genes related to water  
118 balance, metabolism will differ between dry forest and rainforest populations, reflecting local  
119 adaptation to different habitats. With respect to sensory systems, due to higher diversity of flora  
120 and fauna, including colorful fruits presented against green foliage, and increased humidity,  
121 genes underlying color vision (opsin genes) and chemosensation (olfactory and taste receptor  
122 genes) are predicted to be more diverse in rainforest habitats [27–29].

123

## 124 **RESULTS**

125

### 126 **1. Comparative Genomics**

127

#### 128 ***Genome assembly and gene annotation***

129

130 Our reference genome assembly for *Cebus imitator* is comprised of 7,742 scaffolds  
131 (including single contig scaffolds) with an N50 scaffold length of 5.2 Mb and an N50 contig  
132 length of 41 kb. The final ungapped assembly length is 2.6 Gb (GenBank accession:  
133 GCA\_001604975.1). Our estimate of total interspersed repeats using WindowMasker [30]  
134 output is 45.8%. The numbers of annotated genes are 20,740 and 9,556 for protein-coding and  
135 non-coding genes, respectively (Table S1). Measures of gene representation using the known  
136 human RefSeq set of 56,230 transcripts show an average of >94% coverage with a mean  
137 identity of 92.5%. Overall, our draft assembly metrics and gene representation are consistent  
138 with other non-human primate (NHP) short-read reference assemblies [31].

139

#### 140 ***Positive selection analyses***

141

142 We recovered 23,402 Orthologous Groups (OGs). Capuchins share 18,475 OGs with  
143 human, 17,589 OGs with rhesus macaque, 15,582 OGs with mouse, and 14,404 OGs with dog.  
144 When we included orthologous genes that are present simultaneously in all 15 species, we  
145 recovered 7,519 OGs, which we subsequently used in the natural selection analyses ( $d_N/d_S=\omega$ ).  
146 We identified 612 genes under positive selection ( $p<0.05$  after FDR correction) in the *Cebus*  
147 lineage using the branch model. We also performed a branch-site test using codeml in  
148 PAML[32] and identified a second set of 748 genes under positive selection in *Cebus* (Table S2  
149 Sheet 2). The results of our enrichment analysis for biological processes using DAVID [33]

150 identified genes that underlie brain development, sensation, and lifespan, which were of  
151 particular interest given the derived features of capuchin biology (Figure 3).

152

153 *Brain development and longevity*

154

155 Capuchins have the largest brain to body ratio of any monkey, and are known for their  
156 sensorimotor intelligence [7] and derived cognitive abilities [8]. Of the 748 genes identified as  
157 being under positive selection in the branch-site model, 17 were previously associated with  
158 brain development (Table S2, Sheet 6, row 18) and 5 were linked to neurogenesis (Table S2,  
159 Sheet 6, row 116). For example, *WDR62*, *BPTF*, *BBS7*, *NUP113*, mutations are directly  
160 associated with brain size and related malformations, including microcephaly [34–37]. *MTOR*  
161 signaling malfunction is also implicated in developmental brain malformations [38], and *NUP113*  
162 is involved in nuclear migration during mammalian brain development [39]. Several genes are  
163 linked with brain tumor formation (including *ZNF217*), and others with cognitive ability (e.g.  
164 *PHF8* [40]).

165 We found 27 aging-related genes, as identified in the GenAge database [41,42], under  
166 positive selection in capuchins including *PARP1*, *MTOR*, *SREBF1*, *INSR*, *HTT*, *RB1* and *MDM2*  
167 (Table S2, Sheet 7). Of note, poly (ADP-ribose) polymerase 1 (*PARP1*) putatively serves as a  
168 determinant of mammalian aging due to its activity in the recovery of cells from DNA damage. In  
169 previous studies, gene expression levels of *PARP1* were inversely correlated with mammalian  
170 lifespan [43]. Another large body of research has associated the mechanistic target of rapamycin  
171 (*MTOR*) with aging and longevity in various organisms [44], making it a prime candidate for  
172 therapeutic interventions in aging [45]. *MTOR* acts as a regulator of cell growth and proliferation  
173 while also being generally involved in metabolism and other processes. Additional key genes in  
174 aging and metabolism include sterol regulatory element binding transcription factor 1 (*SREBF1*),  
175 which acts as a regulator of the metabolic benefits of caloric restriction [46,47], and the insulin

176 receptor (*INSR*), a major player in longevity regulation [48]. As for specific age-related diseases,  
177 huntingtin (*HTT*) is under selection in mammals; *HTT* is not only involved in Huntington's disease but  
178 has also been associated with longevity in mice [49]. Lastly, various cell cycle regulators (e.g., *RB1*,  
179 *MDM2*) are also under positive selection in capuchins, and indeed, cell cycle is an enriched term  
180 among positively selected genes (Table S2), though these could be related to other life history traits  
181 like developmental schedules that correlate with longevity.

182

## 183 **2. Population Genomics and Local Adaptation**

184

### 185 ***Population structure, genetic diversity, and demographic history in Costa Rican white-*** 186 ***faced capuchins***

187

188         Of the 24 capuchin DNA samples that we sequenced and mapped to our reference  
189 genome, 15 were fecal-derived (Table S3). When comparing the high coverage tissue-derived  
190 genomes from the Santa Rosa site to those generated from our novel application of  
191 fluorescence-activated cell sorting to isolate fecal-sourced cells (fecalFACS), we observed no  
192 substantial difference in quality, coverage, heterozygosity, or GC content (Figures 2, S1, S2,  
193 Supplemental Text). This includes the first (to our knowledge) high-coverage (12.2 X) whole  
194 mammalian genome generated from a fecal sample.

195         The pattern of clustering in our maximum likelihood single nucleotide variant (SNV) tree  
196 recapitulates the expected patterns of geographic distance and ecological separation in our  
197 samples (Figure 4). Likewise, in the projected PCA all individuals from the seasonal dry forests  
198 in the northwest are sharply discriminated from individuals inhabiting the southern rainforests  
199 along PC1. These relationships are not perturbed by depth of coverage, or source material  
200 (tissue-based vs fecalFACS genomic libraries) (Figure 4). Levels of heterozygosity calculated in  
201 overlapping 1 Mb genomic windows (with a step size of 100 kb) were significantly higher in the

202 southern population ( $W = 1,535,400,000$ ,  $p\text{-value} < 2.2e-16$ ; Figure 5A, Figure S3).  
203 Furthermore, the median pairwise heterozygosity for each southern individual (range: 0.00065 -  
204 0.00071) was higher than any northern monkey (0.00047 - 0.00057) ( $W = 0$ ,  $p\text{-value} =$   
205 0.009524; Table S5). In the northern population, we also identified long runs of homozygosity  
206 significantly more often ( $W = 24$ ,  $p\text{-value} = 0.009524$ ), and more of the longest runs ( $\geq 5$  Mb)  
207 ( $W = 1315.5$ ,  $p\text{-value} = 0.03053$ ; Figures 5B, S4, S5). Pairwise sequential Markovian coalescent  
208 (PSMC) analysis of demographic history (Figure 5C) reveals that white-faced capuchins had a  
209 peak effective population size of  $\sim 60,000$  effective individuals  $\sim 1$  mya, which declined to fewer  
210 than 20,000 during the middle to late Pleistocene transition. After recovering during the middle  
211 Pleistocene, they declined precipitously through the late Pleistocene to fewer than 5,000  
212 effective individuals.

213

#### 214 ***Local adaptation to seasonal dry forest biome***

215

216 We predicted that genes related to water balance, metabolism, and sensation would  
217 differ between dry forest and rainforest populations, reflecting local adaptation to different  
218 habitats. To test this, we searched for associations between genes in windows with high  $F_{ST}$  and  
219 divergent non-synonymous SNVs with high or moderate effect. Of the 299 genes identified in  
220 high  $F_{ST}$  windows, 39 had highly differentiated non-synonymous SNVs (Figure S6, Tables S6,  
221 S7). Our enrichment analysis identified a single significant GO biological process: regulation of  
222 protein localization to cilium (GO: 1903564). Remarkably--and in accordance with our  
223 hypothesis--disruptions of cilia proteins are predominantly associated with disorders of the  
224 kidney and retina (ciliopathies) [50]. Furthermore, enrichment of genes associated with disease  
225 states was linked to kidney function, metabolism, and muscular wasting. These genes are good  
226 candidates for adaptive resilience to seasonal water and food shortages and warrant further  
227 investigation. We highlight several genes of particular promise (Figure 6, Figure S7).



228 Evidence of adaptation to food and water scarcity

229

230 Multiple candidate genes indicate that dry-forest capuchins could be adapted to  
231 seasonal drought-like conditions and food scarcity. *SERPINC1* encodes antithrombin III, which  
232 is involved in anticoagulant and anti-inflammatory responses associated with numerous kidney-  
233 related disorders including salt-sensitive hypertension, proteinuria, and nephrotic syndrome [51–  
234 56]. *SERPINC1* is overexpressed in the renal cortex of Dahl salt-sensitive rats fed a high salt  
235 diet [55], suggesting that variants could be facilitating water/salinity balance in the dry-forest  
236 capuchins. Additionally, sequence variants of *AXDND1* (as identified in the GeneCards  
237 database) are associated with nephrotic syndrome, a kidney disorder that commonly presents  
238 with edema and proteinuria. *BCAS3* is expressed in multiple distal nephron cells types [57], and  
239 is associated with four pleiotropic kidney functions (concentrations of serum creatinine, blood  
240 urea nitrogen, uric acid, and the estimated glomerular filtration rate based on serum creatinine  
241 level) [58]. Although we did not identify any population-specific non-synonymous SNVs in  
242 *BCAS3*, the genomic windows encompassing the gene rank among the highest regions of  $F_{ST}$  in  
243 our dataset, and intronic variation in *BCAS3* putatively impacts estimated glomerular filtration  
244 rate in humans [57].

245 The association of *BCAS3* and serum creatinine is of particular interest, given field  
246 observations of capuchins from SSR, whose urinary creatinine levels are associated with  
247 decreased muscle mass during periods of seasonally low fruit availability [59]. Creatinine is a  
248 byproduct of the metabolism of creatine phosphate in skeletal muscle, which is normally filtered  
249 by the kidneys, and can be used as a clinical biomarker of kidney function, chronic kidney  
250 disease [58], and as a monitor of muscle mass [59,60]. Multiple congenital muscular  
251 dystrophies—including mild forms that present with muscular wasting—and abnormal circulating  
252 creatine kinase concentration (HP:0040081) are associated with candidate genes *ITGA7*, *ISPD*  
253 (*CRPPA*), and *SYNE2* [61–64]. Furthermore, transgenic overexpression of *ITGA7* has been

254 shown to reduce muscular pathologies caused by mutations in *LAMA2* [65], which falls in a high  
255  $F_{ST}$  window. The relationship among seasonal resource availability, kidney function, and muscle  
256 mass is further supported by a potential adaptive role in capuchin sugar metabolism and  
257 frugivory. In particular, *GLIS3* is one of two genes known to be associated with type 1 diabetes,  
258 type 2 diabetes, and neonatal diabetes [66], and appears to be diverging between populations.  
259 Additionally, while insulin receptor substrate (*IRS4*) did not fall in a high  $F_{ST}$  window, we  
260 observed a non-synonymous SNP of medium effect fixed between populations. Given the  
261 appearance of both diabetes and kidney disorders in our gene sets, we conducted an a  
262 *posteriori* search of our high  $F_{ST}$  gene set for overrepresentation of genes associated with  
263 diabetic nephropathy (EFO\_0000401) in the GWAS catalogue (Table S6). Seven genes were  
264 present in both our gene set of 299 high  $F_{ST}$  genes and the diabetic nephropathy set of 117.  
265 Given the 16,553 annotated genes with HGNC Gene IDs, seven overlapping genes would occur  
266 with  $p = 0.00046$  when permuted 100,000 times. We take this as promising evidence that these  
267 genes have been under selection in the northwestern population.

268

### 269 Evidence of adaptation in sensory systems

270

271         Given the ecological differences between the northern dry and southern wet forests, we  
272 predicted that the evergreen, humid environment of the lowland rainforest would favor enhanced  
273 diversity of both color vision (opsin genes) and olfaction (olfactory receptor genes) would result  
274 in population specific variation in chemosensory and visual genes. We did not find support for  
275 this; in both populations, we observed similar polymorphism at each of the three medium/long  
276 wave cone opsin tuning sites (180, A/S; 277, F/Y; and 285, T/A) (Table S8). None of these  
277 codons is a novel variant [67,68], providing no support for the hypothesis of differences in the  
278 perception of photopic (cone-driven) vision between the two biomes. However, we did observe  
279 some evidence for population specific variation associated with the photoreceptive layers of the

280 retina. First, creatine kinase plays an important role in providing energy to the retinal pigment  
281 epithelium [69]. Secondly, we identified a fixed non-synonymous SNV in *CCDC66*, which falls in  
282 a high  $F_{ST}$  region and is heavily expressed in photoreceptive layers of the retina.  
283 Electroretinography of *CCDC66* *-/-* mice reveals a significant reduction in scotopic (rod-driven)  
284 photoreceptor response [70], indicating a potential effect on vision in low-light conditions.  
285 Curiously, *CCDC66* *-/-* mice, also display neurodegeneration of the olfactory bulb, and have  
286 reduced odor discrimination performance of lemon smells [71]. Turning to olfaction, we identified  
287 614 olfactory receptor (OR) genes and pseudogenes in the capuchin reference genome (408  
288 intact, 45 truncated, and 161 pseudogenized (Table S9). To test for population differences in the  
289 OR gene repertoire, we assembled each olfactory gene/pseudogene independently in each  
290 individual. The proportion of total functional ORs was stable across individuals and populations,  
291 with trivial fluctuations (North  $\bar{x}$  = 411,  $s$  = 1.6; South  $\bar{x}$  = 408.5,  $s$  = 1.3), possibly driven by a  
292 small difference in OR family 5/8/9 (Table S10). We also identified 8 vomeronasal and 28 taste  
293 receptor and taste receptor-like genes (Table S11), two of which (*TAS1R* and *TAS2R4*) have  
294 non-synonymous SNVs with fixed variants in the north (Table S12). The functional significance  
295 of these variants is unknown, but may be revealed via cellular expression systems in future  
296 research [72].

297

## 298 **DISCUSSION**

299

### 300 **Comparative genomics of white-faced capuchins**

301

302 Among primates, capuchin monkeys are known for their relatively large brains, cognitive  
303 capacity, and sensorimotor intelligence [7,8,73,74]. Accordingly, it is perhaps unsurprising to  
304 see positive selection in the *Cebus* lineage and evidence of shifts in gene function linked to  
305 brain function and development relative to other primates. In particular, positive selection in

306 *WDR62*, *BPTF*, *BBS7*, *NUP133*, and *MTOR*, and *PHF8* supports our hypothesis that the  
307 capuchin lineage has undergone adaptation linked to brain development. The association of  
308 several of these genes with size related brain malformations [34–37], such as microcephaly,  
309 suggests that they could be influencing the large relative brain size of capuchins. Furthermore,  
310 the evidence of selection in *PHF8*, which is associated with human cognitive capacity, aligns  
311 with the link between brain size and intelligence that has been observed in other primates [75].  
312 While we highlight here the putative functional roles of these genes, which are based on clinical  
313 studies and comparative genomics, we acknowledge that further examination of their function in  
314 the context of capuchin biology is warranted.

315 In the context of longevity, it is noteworthy that we observed genes under selection  
316 associated with DNA damage response, metabolism, cell cycle and insulin signaling [76]. Of  
317 particular interest are: *PARP1*, *MTOR*, *SREBF1*, *INSR1*, and *HTT*. Damage to the DNA is  
318 thought to be a major contributor to aging [77]. Previous studies have also shown that genes  
319 involved in DNA damage responses exhibit longevity-specific selection patterns in mammals  
320 [41]. It is therefore intriguing that *PARP1*, a gene suggested to be a determinant of mammalian  
321 aging [43], is under selection in capuchins. Other genomes of long-lived mammals also revealed  
322 genes related to DNA repair and DNA damage responses under selection [78,79]. In the context  
323 of longevity, it is also noteworthy that we observed genes under selection associated with  
324 metabolism, cell cycle and insulin signaling. Other genome sequencing efforts of long-lived  
325 mammals also revealed changes in such pathways [79,80]. Intriguingly, short-lived species also  
326 exhibit genes under selection related to insulin receptors, raising the possibility that the same  
327 pathways associated with aging in model organisms are involved in the evolution of both short-  
328 and long lifespans [81], an idea supported by our results. Of course, because aging-related  
329 genes often play multiple roles, for example in growth and development, it is impossible to tell  
330 for sure whether selection in these genes is related to aging or to other life-history traits, like  
331 growth rates and developmental times, that in turn correlate with longevity [82]. Therefore,

332 although we should be cautious about the biological significance of our findings, it is tempting to  
333 speculate that, like in other species, changes to specific aging-related genes or pathways, could  
334 contribute to the longevity of capuchins.

335

### 336 **Population genomics and local adaptation with fecalFACS**

337

338 Through a novel use of flow cytometry/FACS, we have developed a new method for the  
339 isolation of epithelial cells from mammalian feces for population genomics. We generated the  
340 first high-coverage, minimally biased mammalian genome solely from feces. Additionally, we  
341 have demonstrated that fecalFACS can be used to generate low coverage SNP datasets that  
342 are suitable for population assignment and clustering. FecalFACS is cost-effective and  
343 minimizes the biases that commonly occur in traditional bait-and-capture approaches to the  
344 enrichment of endogenous DNA from feces. Furthermore, fecalFACS does not require costly  
345 impractical preservation of biomaterial in liquid nitrogen; rather, we rely on room-temperature  
346 stable storage in RNAlater. FecalFACS offers great benefits to the field of mammalian  
347 conservation and population genomics.

348 White-faced capuchins are the most northerly distributed member of the Cebinae, having  
349 dispersed over the isthmus of Panama in a presumed speciation event with *C. capucinus* in  
350 South America ~1.6 mya [13–15]. After expanding during the early late Pleistocene, white-faced  
351 capuchins appear to have undergone a dramatic reduction in effective population size. This  
352 pattern predates the movement of humans into Central America, and could reflect a series of  
353 population collapses and expansions caused by glacial shifts and fluctuating forest cover  
354 availability during the Pleistocene. At a finer scale, we observed a clear demarcation between  
355 the northern dry- and southern wet-forest populations in Costa Rica. Higher levels of  
356 heterozygosity in the south and lower levels in the northwest are in accordance with the  
357 hypothesis that capuchins dispersed northwards across Costa Rica. White-faced capuchins in

358 SSR are near the northernmost limits of their range, which extends as far north as Honduras,  
359 and we predict they may represent some of the least genetically diverse members of their  
360 species. Given the limitations of the available sampling sites, it is possible that the appearance  
361 of an ecological divide is actually evidence of isolation by distance; however, given that the  
362 single individual from Cañas clusters closely with the individuals from SSR, despite a  
363 geographic distance of more than 100 km, we suggest that isolation by distance does not  
364 completely explain the population differentiation.

365 We found evidence that the recent northern expansion of *Cebus imitator* has undergone  
366 local adaptation to the extreme seasonality of rainfall and food availability. The effects of  
367 seasonality have been linked to biological consequences for Costa Rican white-faced capuchins  
368 in other contexts. Seasonal fluctuations in food abundance and rainfall are associated with  
369 compositional changes in the gut microbiome of capuchins at SSR [83], which differs markedly  
370 from that observed in capuchins inhabiting nonseasonal forests [84]. Previous capuchin  
371 research in the dry forest also demonstrates seasonal negative energy balance and periods of  
372 pronounced muscle loss through catabolic processes [59]. These observations fit with the notion  
373 that animals living in seasonal environments, or pursuing seasonal migrations, are more likely to  
374 have weight fluctuations through binge-subsist cycles that map onto food abundance [85].  
375 Accordingly, we observed population-specific variation in genes implicated in water/salt balance,  
376 kidney function, muscle wasting, and metabolism (e.g. *SERPINC1*, *BCAS3*, *ITGA7*, *ISPD*, and  
377 *GLIS3*). In light of this, we contend that seasonal drought and food shortages would create an  
378 environment favoring efficient catabolism when needed and adaptations for maintaining water  
379 balance. Given that selection operates on both gene function and regulation, we suspect the  
380 observed variation is affecting gene expression or enzymatic efficiency, which offers a  
381 promising avenue for future research.

382 Additionally, we found evidence of 408 OR genes, 28 TASR, and 7 VR genes that are  
383 putatively functional. These numbers are similar to, or slightly higher than, the number of

384 chemosensory genes identified in other anthropoid primates [86–90]. The VR gene repertoire of  
385 capuchins highlights the persistent role of the vomeronasal organ that is used in social  
386 communication of other mammals, but that has been nearly lost from all African and Asian  
387 monkeys [89]. Like most other primates in the Americas, capuchins possess an intriguing color  
388 vision system characterized by extensive intraspecific genotypic and phenotypic variation [32–35].  
389 Contrary to our prediction, dry-forest and rainforest capuchins have similar numbers of color  
390 vision, taste and olfactory receptors. This indicates that there are not greater numbers of  
391 functional sensory genes in areas of higher vegetative biodiversity or humidity. The tuning of the  
392 chemosensory receptors may vary between habitat types and may be elucidated by future work.  
393 While we did observe population-specific variation in *CCDC66*, which is expressed in  
394 photoreceptive layers of the retina and may affect odor discrimination, the ecological  
395 significance of this result, if any, is unclear at present but may warrant future attention.

396

## 397 **CONCLUSION**

398

399 We provide the first annotated reference assembly for a capuchin monkey. We observed  
400 evidence of selection in *C. imitator* on genes involved with brain function and cognitive capacity.  
401 These results are in accordance with the remarkably long life span, large brain, and high degree  
402 of sensorimotor intelligence that has been observed in capuchins. These genes are good  
403 candidates for further investigation of traits which have evolved in parallel in apes and other  
404 mammals. Through a novel use of flow cytometry/FACS, we developed a new method for the  
405 isolation of epithelial cells from mammalian feces for population genomics. FecalFACS allowed  
406 us to generate both the first high-coverage, minimally biased mammalian genome solely from  
407 feces, as well as low coverage SNV datasets for population level analyses. In our population  
408 level analysis of wet- and dry-forest capuchins, we observed both evidence of population  
409 structure between and local adaptation to these different habitats. In particular, we identified

410 selection in genes related to food and water scarcity, as well as muscular wasting, all of which  
411 have been observed during seasonal extremes in the dry forest population.

412

## 413 **METHODS**

414

### 415 Study populations and sample collection

416 Central American white-faced capuchins (*Cebus imitator*), a member of the gracile  
417 radiation of capuchins (genus *Cebus*) [91], were recently recognized as a species, distinct from  
418 *C. capucinus* in South America [14]. *Cebus imitator* occupies a wide diversity of habitats,  
419 spanning lowland rainforests and cloud forests in Panama and throughout southern, eastern,  
420 and central Costa Rica, and tropical dry forests in northwestern Costa Rica and Nicaragua. The  
421 annual precipitation and elevation of rainforest versus dry forest biomes in their current range  
422 vary dramatically, leading to considerable variation in the resident flora and fauna [92,93]. We  
423 sampled individual Costa Rican capuchin monkeys from populations inhabiting two distinct  
424 habitats. 1) lowland rainforest around Quepos, Puntarenas Province; and 2) tropical dry forest at  
425 two sites in Guanacaste Province. In total, we collected samples from 23 capuchins, a list of  
426 which is provided in table S3.

427 We sampled capuchins inhabiting a lowland tropical rainforest biome by collaborating  
428 with *Kids Saving the Rainforest* (KSTR) in Quepos, Costa Rica. We acquired blood samples  
429 from 4 wild capuchins from nearby populations who were undergoing treatment at the facility  
430 (although we were unable to collect paired fecal samples). For one of these individuals, an adult  
431 male white-faced capuchin that was mortally wounded by a vehicle in Costa Rica, we  
432 additionally sampled tissues from several organs. DNA derived from the kidney was used for the  
433 reference genome assembly.

434 We collected 21 samples from 19 individuals in the northern tropical dry forest. 16 fecal  
435 samples and 4 tissue samples were from free-ranging white-faced capuchin monkeys (*Cebus*



436 *imitator*) at in the Sector Santa Rosa (SSR), part of the Área de Conservación Guanacaste in  
437 northwestern Costa Rica, which is a 163,000 hectare tropical dry forest nature reserve (Figure  
438 1). Behavioral research of free-ranging white-faced capuchins has been ongoing at SSR since  
439 the 1980's which allows for the reliable identification of known individuals from facial features  
440 and bodily scars [94]. The 16 fresh fecal samples were collected from 14 white-faced capuchin  
441 monkeys immediately following defecation (Table S3). We placed 1 mL of feces into conical 15  
442 mL tubes pre-filled with 5 mL of RNAlater. RNAlater preserved fecal samples were sent to the  
443 University of Calgary, where they were stored at room temperature for up to three years. To  
444 evaluate other preservation methods, we also collected two additional capuchin monkey fecal  
445 samples (SSR-FL and a section of SSR-ML), which we stored in 1X PBS buffer and then frozen  
446 in liquid nitrogen with a betaine cryopreservative [95]. Given the logistical challenges of carrying  
447 liquid nitrogen to remote field sites, we prioritized evaluation of samples stored in RNAlater. We  
448 also collected tissue and blood samples opportunistically. During the course of our study, 4  
449 individual capuchin monkeys died of natural causes at SSR, from whom we were able to collect  
450 tissue samples, which were stored in RNAlater. Additionally, we collected a blood sample from 1  
451 northern dry-forest individual housed at KSTR that originated near the town of Cañas, which is  
452 ~100 km southwest of SSR.

453

#### 454 Genome-wide sequencing, genome assembly and gene annotation

455 We assembled a reference genome for *Cebus imitator* from DNA extracted from the  
456 kidney of a male Costa Rican individual (KSTR64) using a short read approach (Illumina HiSeq  
457 2500). Based on a genome estimate of 3 Gb, the total sequencing depth generated was 81X,  
458 including 50X of overlapping read-pairs (200 bp insert), 26X and 5X of 3 and 8 kbs insert read  
459 pairs, respectively. The combined sequence reads were filtered and assembled using default  
460 parameter settings with ALLPATHS-LG [96]. To improve the quality of gene annotation, we  
461 isolated total RNA from the whole blood of an adult male white-faced capuchin (ID: CNS-HE)

462 permanently residing at the KSTR wildlife rehabilitation center. The blood was immediately  
463 stored in a PAXgene blood RNA tube (Qiagen), and frozen at ultralow temperatures for  
464 subsequent use. To extract total RNA, we used the PAXgene Blood RNA kit following the  
465 manufacturer's recommended protocols. A RiboZero library construction protocol was followed  
466 according to the manufacturer's specifications and sequenced on an Illumina HiSeq 2000  
467 instrument creating 150 bp paired-end reads. We assembled the FASTQ sequence files into  
468 transcripts with Trinity, and submitted the assembled transcriptome to the National Center for  
469 Biotechnology Information (NCBI) to assist in gene annotation. The capuchin genome assembly  
470 was annotated with the NCBI pipeline previously described here:

471 (<http://www.ncbi.nlm.nih.gov/books/NBK169439/>).

472

#### 473 Phylogenetic arrangement and data treatment

474 The phylogenetic arrangement in this study included 14 species as outgroups to *C.*  
475 *imitator*: three Platyrrhini (*Callithrix jacchus*, *Aotus nancymae*, *Saimiri boliviensis*), six  
476 Catarrhini (*Macaca mulatta*, *Rhinopithecus roxellana*, *Nomascus leucogenys*, *Pan troglodytes*,  
477 *Homo sapiens*, *Pongo abelii*), one Strepsirrhini (*Microcebus murinus*), one rodent (*Mus*  
478 *musculus*), and three Laurasiatheria (*Canis lupus familiaris*, *Bos taurus*, and *Sus scrofa*).  
479 Genomic cds were downloaded from Ensembl and NCBI (Table S13). The sequences per  
480 genome were clustered using CD-HITest version 4.6 [97] with a sequence identity threshold of  
481 90% and an alignment coverage control of 80%. To remove low quality sequences and keep the  
482 longest transcript per gene, we used TransDecoder.LongOrfs and TransDecoder.Predict  
483 (<https://transdecoder.github.io>) with default criteria.

484

#### 485 Orthology identification

486 The orthology assessment was performed with OMA stand-alone v. 2.3.1 [98]. The OMA  
487 algorithm makes strict pairwise "all-against-all" sequence comparisons and identifies the

488 orthologous pairs (genes related by speciation events) based on evolutionary distances. These  
489 orthologous genes were clustered into Orthologous Groups (OGs). All OGs included one  
490 ortholog sequence from capuchin and at least one outgroup. The tree topology was obtained  
491 from TimeTree (<http://www.timetree.org/>). We identified 7,519 OGs present among the 15  
492 species. Each orthogroup shared by all species was translated into amino acids using the  
493 function `pxtlate -s` in `phyx` [99]. Amino acid sequences were aligned using the L-INS-i algorithm  
494 from MAFFT v.7 [100]. We generated codon alignments using `pxaa2cdn` in `phyx`. To avoid false  
495 positives in low quality regions, the codon alignments were cleaned with the `codon.clean.msa`  
496 algorithm in `rphast` [101], using human as a reference sequence. We used conservative  
497 methodologies of homology and data cleaning to obtain a smaller number of orthologous genes  
498 that avoided false positives with high confidence.

499

500 Positive natural selection analysis through codon-based models of evolution and enrichment  
501 tests

502 To evaluate signals consistent with positive selection in the *C. imitator* genome, we  
503 explored variation in the ratio of non-synonymous and synonymous substitutions ( $d_N/d_S=\omega$ ) in  
504 the ancestor of *Cebus*. We used branch and branch-site substitution models with a maximum  
505 likelihood approach in PAML v4.9 [32], which we implemented through the python framework  
506 ETE-toolkit with the `ete-evol` function [102]. We compared the null model where the omega ( $\omega$ )  
507 value in the branch marked as foreground was set with 1, with the model where the  $\omega$  value was  
508 estimated from the data [103]. Likelihood ratio tests (LRT) were used to test for significance  
509 between the models and probability values were adjusted with a false discovery rate correction  
510 for multiple testing with a q-value  $< 0.05$  for the two positive selection models (branch and  
511 branch-site).

512 We performed functional annotation analysis using DAVID bioinformatics resources -  
513 DAVID 6.7 [33], to ascertain which ontology processes the genes with signals of positive

514 selection were involved. We focussed the enrichment analysis on two functional categories:  
515 Biological Processes (BP) and Genetic Association Database (GAD). GAD is a database from  
516 complex diseases and disorders in humans. Finally, the genes with positive section signal were  
517 intersected with the GenAge database (build 19,307 genes) [42].

518

### 519 FACS

520 Before isolating cells by fluorescence-activated cell sorting, fecal samples were prepared  
521 using a series of washes and filtration steps. Fecal samples were vortexed for 30 s and  
522 centrifuged for 30 s at 2,500 g. Then the supernatant was passed through a 70  $\mu$ m filter into a  
523 50 mL tube and washed with DPBS. After transferring the resultant filtrate to a 15 mL tube, it  
524 was centrifuged at 1,500 RPM for 5 minutes to pellet the cells. Then we twice washed the cells  
525 with 13 mL of DPBS. We added 500  $\mu$ L of DPBS to the pellet and re-filtered through a 35  $\mu$ m  
526 filter into a 5 mL FACS tube. We prepared a negative control (to control for auto-fluorescence)  
527 with 500  $\mu$ L of DPBS and one drop of the cell solution. To the remaining solution, we added 1  
528  $\mu$ L of AE1/AE3 Anti-Pan Cytokeratin Alexa Fluor® 488 antibody or TOTO-3 DNA stain, which  
529 we allowed to incubate at 4°C for at least 30 minutes.

530 We isolated cells using a BD FACSAria™ Fusion (BD Biosciences) flow cytometer at the  
531 University of Calgary Flow Cytometry Core. To sterilize the cytometer's fluidics before  
532 processing each sample, we ran a 3% bleach solution through the system for four minutes at  
533 maximum pressure. We assessed background fluorescence and cellular integrity by processing  
534 the negative control sample prior to all prepared fecal samples. For each sample we first gated  
535 our target population by forward and side scatter characteristics that were likely to minimize  
536 bacteria and cellular debris (Figure S8). Secondary and tertiary gates were implemented to  
537 remove cellular agglomerations. Finally, we selected cells with antibody or DNA fluorescence  
538 greater than background levels. In cases when staining was not effective, we sorted solely on  
539 the first three gates. Cells were pelleted and frozen at -20°C.

540

541 DNA Extraction and Shotgun Sequencing

542 We extracted fecal DNA (fDNA) with the QIAGEN DNA Micro kit, following the “small  
543 volumes of blood” protocol. To improve DNA yield, we increased the lysis time to three hours,  
544 and incubated 50 µL of 56°C elution buffer on the spin column membrane for 10 minutes. DNA  
545 concentration was measured with a Qubit fluorometer. Additionally, to calculate endogenous  
546 DNA enrichment, we extracted DNA directly from five fecal samples prior to their having  
547 undergone FACS. We extracted DNA from the nine tissue and blood samples using the  
548 QIAGEN Genra Puregene Tissue kit and DNeasy blood and tissue kit, respectively.  
549 For the fecal samples, DNA was fragmented to 350 bp with a Covaris sonicator. We built whole  
550 genome sequencing libraries with the NEB Next Ultra 2 kit using 10-11 PCR cycles. Fecal  
551 genomic libraries were sequenced on an Illumina NextSeq (2x150 PE) at the University of  
552 Calgary genome sequencing core and an Illumina HighSeq 4000 at the McDonnell Genome  
553 Institute at Washington University in St. Louis (MGI). Using ½ of one HiSeq 4000 lane, we  
554 achieved an average coverage of 12.2X across the *Cebus imitator* 1.0 genome (sample SSR-  
555 ML). Other fecal samples were sequenced to average depths of 0.1-4.4X (Table S4). High-  
556 coverage (10.3-47.6X), whole genome shotgun libraries were prepared for the blood and tissue  
557 DNA samples and sequenced on an Illumina X Ten system at MGI. For population analyses  
558 within capuchins, we mapped genomic data from all 23 individuals sequenced (Table S3) to the  
559 reference genome.

560

561 Mapping and SNV Generation

562 Reads were trimmed of sequencing adaptors with Trimmomatic [104]. Subsequently, we  
563 mapped the *Cebus* reads to the *Cebus imitator* 1.0 reference genome (GCF\_001604975.1) with  
564 BWA mem [105] and removed duplicates with Picard Tools  
565 (<http://broadinstitute.github.io/picard/>) and SAMtools [106]. We called SNVs for each sample

566 independently using the *Cebus* genome and the GATK UnifiedGenotyper pipeline (*-out\_mode*  
567 *EMIT\_ALL\_SITES*) [107]. Genomic VCFs were then combined using GATK's CombineVariants  
568 restricting to positions with a depth of coverage between 3 and 100, mapping quality above 30,  
569 no reads with mapping quality zero, and variant PHRED scores above 30. Sequencing reads  
570 from one of the high coverage fecal samples (SSR-FL) bore a strong signature of human  
571 contamination (16%), and were thus excluded from SNV generation. We included reads from  
572 nine tissue/blood samples and one frozen fecal sample with high coverage (SSR-ML). In total,  
573 we identified 4,184,363 SNVs for downstream analyses.

574 To remove potential human contamination from sequenced libraries, we mapped  
575 trimmed reads to the *Cebus imitator* 1.0 and human (hg38) genomes simultaneously with  
576 BBsplit [108]. Using default BBsplit parameters, we binned separately reads that mapped  
577 unambiguously to either genome. Ambiguously mapping reads (i.e. those mapping equally well  
578 to both genomes) were assigned to both genomic bins, and unmapped reads were assigned to  
579 a third bin. We calculated the amount of human genomic contamination as the percentage of  
580 total reads unambiguously mapping to the human genome (Table S4). After removing  
581 contaminant reads, all libraries with at least 0.5X genomic coverage were used for population  
582 structure analysis.

583 In order to test the effect of fecalFACS on mapping rates, we selected five samples at  
584 random (SSR-CH, SSR-NM, SSR-LE, SSR-PR, SSR-SN) to compare pre- and post-FACS  
585 mapping rates. To test for an increase in mapping percentage, we ran a one-sample paired  
586 Wilcoxon signed-rank test on the percentages of reads that mapped exclusively to the *Cebus*  
587 genome before and after FACS. Additionally, we ran Pearson's product moment correlations to  
588 test for an effect of the number of cells (log10 transformed) on rates of mapping, read  
589 duplication, and nanograms of input DNA. The above tests were all performed in R.

590

591 *High coverage fecal genome comparison*

592 We made several comparisons between our high-coverage feces-derived genome and  
593 the blood/tissue-derived genomes using window-based approaches. For each test, the feces-  
594 derived genome should fall within the range of variation for members of its population of origin  
595 (SSR). Deviations from this, for example all fecal genomes clustering together, would indicate  
596 biases in our DNA isolation methods. To assess this, we constructed 10 KB windows with a 4KB  
597 slide along the largest scaffold (21,314,911 bp) in the *C. imitator* reference genome. From these  
598 windows, we constructed plots of coverage density and the distribution of window coverage  
599 along the scaffold. Secondly, we assessed the level of heterozygosity in 1 MB / 200 KB sliding  
600 windows throughout the ten largest scaffolds. For each high-coverage genome, we plotted the  
601 density distribution of window heterozygosity. We measured genome-wide GC content with the  
602 Picard Tools CollectGcBiasMetrics function. The percentage of GC content was assessed  
603 against the distribution of normalized coverage and the number of reads in 100 bp windows per  
604 the number reads aligned to the windows.

605

### 606 Population Structure

607 Given the large degree of difference in coverage among our samples, (less than 1X to  
608 greater than 50X), we performed pseudodiploid allele calling on all samples. For each library, at  
609 each position in the SNV set, we selected a single, random read from the sequenced library.  
610 From that read, we called the variant information at the respective SNV site for the given library.  
611 In so doing, we generated a VCF with a representative degree of variation and error for all  
612 samples.

613 To assess population structure and infer splits between northern and southern groups of  
614 Costa Rican white-faced capuchins, we constructed principal components plots with  
615 EIGENSTRAT [109] and built population trees with TreeMix [110]. Because we ascertained  
616 variants predominantly with libraries that were of tissue/blood origin, we built principal  
617 components solely with SNVs from these libraries and projected the remaining fecal libraries

618 onto the principal components. For our maximum likelihood trees, we used two outgroups  
619 (*Saimiri sciureus*, and *Cebus albifrons*), with *S. sciureus* serving as the root of the tree. Given  
620 the geographic distance and anthropogenic deforestation between northern and southern  
621 populations, we assumed no migration. To account for linkage disequilibrium, we grouped SNVs  
622 into windows of 1,000 SNVs. Population size history was inferred from the highest coverage  
623 non-reference individual, SSR-RM08 with PSMC [111], using default parameters  
624 (<https://github.com/lh3/psmc>).

625

### 626 Local adaptation, $F_{ST}$ , heterozygosity, relatedness

627 For all analyses of local adaptation and heterozygosity between populations, we  
628 excluded individuals from our low coverage dataset. We tested for the degree of relatedness  
629 among all high and low coverage individuals using READ [112] and identified two of the high-  
630 coverage individuals from SSR, SSR-ML and SSR-CR, as potential first degree relatives (Figure  
631 S9, Table S14). For all statistical analyses of high-coverage samples, we removed SSR-ML,  
632 because SSR-CR was sequenced to higher average depth.

633 For each individual, we calculated heterozygosity in 1 Mb / 200 Kb sliding windows  
634 across the genome for all scaffolds at least 1 Mb in length. Windows were generated with  
635 BedTools windowMaker [113] and heterozygosity was calculated as the per-site average within  
636 each window. Based upon a visual inspection of the average heterozygosity values across the  
637 genome (Figure 5), we classified a window as part of a run of homozygosity if the window's  
638 average heterozygosity fell below 0.0002. Descriptive statistics and two-sided Wilcoxon tests  
639 were calculated in R.

640 For each high-coverage sample, we calculated the Hudson's  $F_{ST}$  ratio of averages [114]  
641 in 20 kb windows with a slide of 4 Kb across the genome. Among the genes present in each  
642 window in the top 0.5% and top 0.1% of  $F_{ST}$  values, we searched for SNPs with high or  
643 moderate effects using SnpEff and identified those SNPs with high  $F_{ST}$  values ( $> 0.75$ ) using



644 VCFtools. We searched for functional enrichment of our population gene set using ToppFun in  
645 the ToppGene Suite [115]. In an effort to identify candidate genes for further investigation, we  
646 set low thresholds for significance (FDR p-value < 0.1 and the minimum number of genes per  
647 category to 1).

648

#### 649 Chemosensory genes

650 The chemosensory behaviors of capuchins have been well-studied [31], and taste and  
651 olfaction are suspected to play an important role in their foraging ecology. 614 orthologous olfactory  
652 receptor genes were identified in the *Cebus* reference genome using previously described  
653 methods [116]. Briefly, putative OR sequences were identified by conducting TBLASTN  
654 searches against the capuchin reference assembly using functional human OR protein  
655 sequences as queries with an e-value threshold of 1e-20. For each reference-derived OR gene,  
656 we added 500 bp of flanking sequence to both the 5' and 3' ends in a bed file. For each  
657 individual, we extracted the OR gene region from the gVCF and generated a consensus  
658 sequence defaulting to the reference allele at variable site using bcftools [117]. The number of  
659 intact, truncated, and pseudogenized OR genes in each individual were identified using the  
660 ORA pipeline [118]. We considered an OR gene to be putatively functional if its amino acid  
661 sequence was at least 300 amino acids in length. ORA was further used to classify each OR  
662 into the appropriate class and subfamily with an e-value cutoff of 1e-10 to identify the functional  
663 OR subgenome for each individual [118,119]. Taste and vomeronasal receptor genes were  
664 identified in the NCBI genome annotation, and variable positions were located by scanning the  
665 VCF with VCFtools [120] and bash. The positions of *Cebus* opsin tuning sites have been  
666 identified previously [68]. With the high-coverage dataset, we identified the allele(s) present at  
667 each locus in the VCF. For each low-coverage fecal-derived genome, we located the position of  
668 the tuning site in the bam file using SAMtools [117] tview and manually called the variant when  
669 possible.

670

671 **DECLARATIONS**

672

673 **Ethics approval and consent to participate**

674

675 This research adhered to the laws of Costa Rica, the United States, and Canada and  
676 complied with protocols approved by the Área de Conservación Guanacaste and by the Canada  
677 Research Council for Animal Care through the University of Calgary's Life and Environmental  
678 Care Committee (ACC protocol AC15-0161). Samples were collected with permission from the  
679 Área de Conservación Guanacaste (ACG-PI-033-2016) and CONAGEBIO (R-025-2014-OT-  
680 CONAGEBIO; R-002-2020-OT-CONAGEBIO). Samples were exported from Costa Rica under  
681 permits from CITES and Area de Conservacion Guanacaste (2016-CR2392/SJ #S 2477, 2016-  
682 CR2393/SJ #S 2477, DGVS-030-2016-ACG-PI-002-2016; 012706) and imported with  
683 permission from the Canadian Food and Inspection Agency (A-2016-03992-4).

684

685 **Consent for Publication**

686

687 Not applicable

688

689 **Availability of data and materials**

690

691 The reference genome is available at NCBI through BioProjects PRJNA298580 and  
692 PRJNA328123. RNAseq reads used in genome annotation can be accessed through  
693 PRJNA319062. The sequencing reads used in the local adaptation will be released by NCBI  
694 upon publication (PRJNA610850), and are available immediately to reviewers and editors upon  
695 request from the corresponding author.

696

697 **Competing Interests**

698

699 The authors declare that they have no competing interests.

700

701 **Funding**

702

703 Funding was provided by Washington University in St. Louis, the Canada Research  
704 Chairs Program, and a National Sciences and Engineering Council of Canada Discovery grant  
705 (to A.D.M.), the Alberta Children's Hospital Research Institute (to A.D.M. and J.D.O), the Beatriu  
706 de Pinós postdoctoral programme of the Government of Catalonia's Secretariat for Universities  
707 and Research of the Ministry of Economy and Knowledge (to J.D.O), and the Japan Society for  
708 the Promotion of Science 15H02421 and 18H04005 (S.K.). This work was partly funded by a  
709 Methuselah Foundation grant to J.P.M. To the Comisión Nacional de Investigación Científica y  
710 Tecnológica (CONICYT) - Chile through the doctoral studentship number N°21170433 and the  
711 scholarship from MECESUP AUS 2003 to D.T.M. GenAge is funded by a Biotechnology and  
712 Biological Sciences Research Council (BB/R014949/1) grant to J.P.M. TMB is supported by  
713 BFU2017-86471-P (MINECO/FEDER, UE), Howard Hughes International Early Career, Obra  
714 Social "La Caixa" and Secretaria d'Universitats i Recerca and CERCA Programme del  
715 Departament d'Economia i Coneixement de la Generalitat de Catalunya (GRC 2017 SGR 880).  
716 C.F is supported by "La Caixa" doctoral fellowship program. EL is supported by CGL2017-  
717 82654-P (MINECO/FEDER, UE). The funding bodies played no role in the design of the study,  
718 in the collection, analysis, and interpretation of data, or in writing the manuscript.

719

720

721

722 **Author contributions**

723

724 ADM and JDO conceived of the project

725 JDO, ADM, YN, WCW, RK, JdC, JPM, and TMB contributed to the study design

726 JDO, DTM, MdM, MJM, LFK, and MCJ performed computational analyses

727 JDO, RK, and JT conducted flow cytometry

728 JDO, ADM, CF, JH, and EL conducted molecular lab work

729 ADM, GHP, ADF, JAH, and SK contributed samples

730 ADM, RK, and TMB provided computational and laboratory resources

731 JDO, ADM, MJM, JPM, and DTM wrote the manuscript with commentary from all authors

732

733

734 **Acknowledgements**

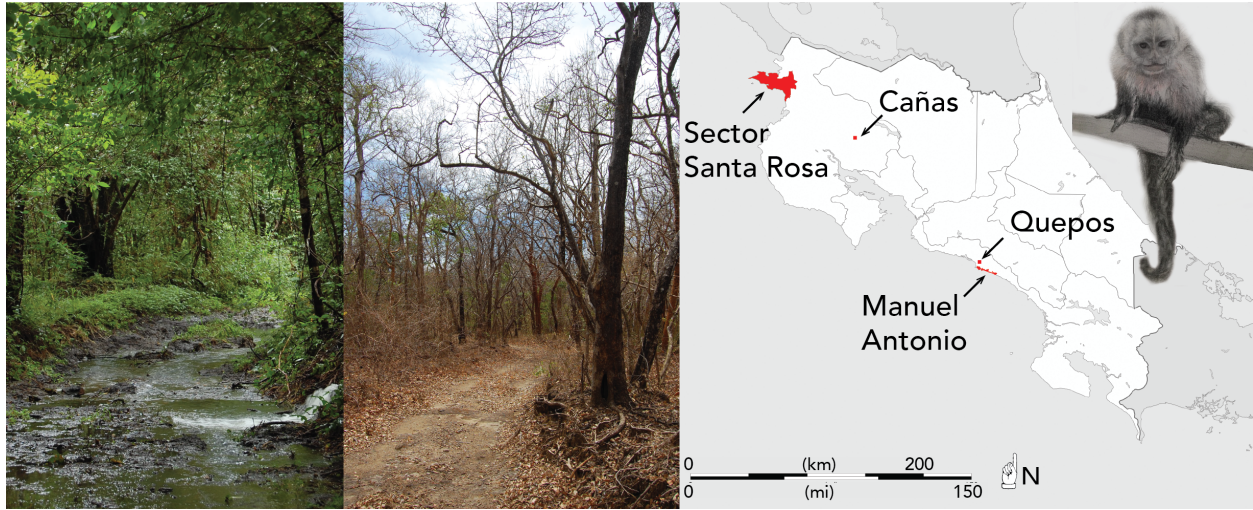
735

736 We thank R. Blanco Segura and M. M. Chavarria and staff from the Área de  
737 Conservación Guanacaste and Ministerio de Ambiente y Energía. From Kids Saving the  
738 Rainforest we thank the volunteers and veterinarians, especially Pia Martin, Carmen Soto,  
739 Jennifer Rice and Chip Braman. For assistance in the lab, we acknowledge Kelly Kries, Gwen  
740 Duytschaever, Jene Weatherhead, Laurie Kennedy, and Yiping Liu. We thank Aoife Doherty  
741 and Mengjia Li for exploratory analyses of selection in aging-related genes and acknowledge  
742 Patrick Minx and Kim Kyung for assistance with bioinformatics. We also thank Jessica Lynch  
743 and Hazel Byrne for comparative data. Thanks to R. Gregory in the Centre for Genomic  
744 Research and I.C. Smith in the Advanced Research Computing at the University of Liverpool for  
745 the access to the computing resources. To Dr. J.C Opazo for the insightful discussion.

746

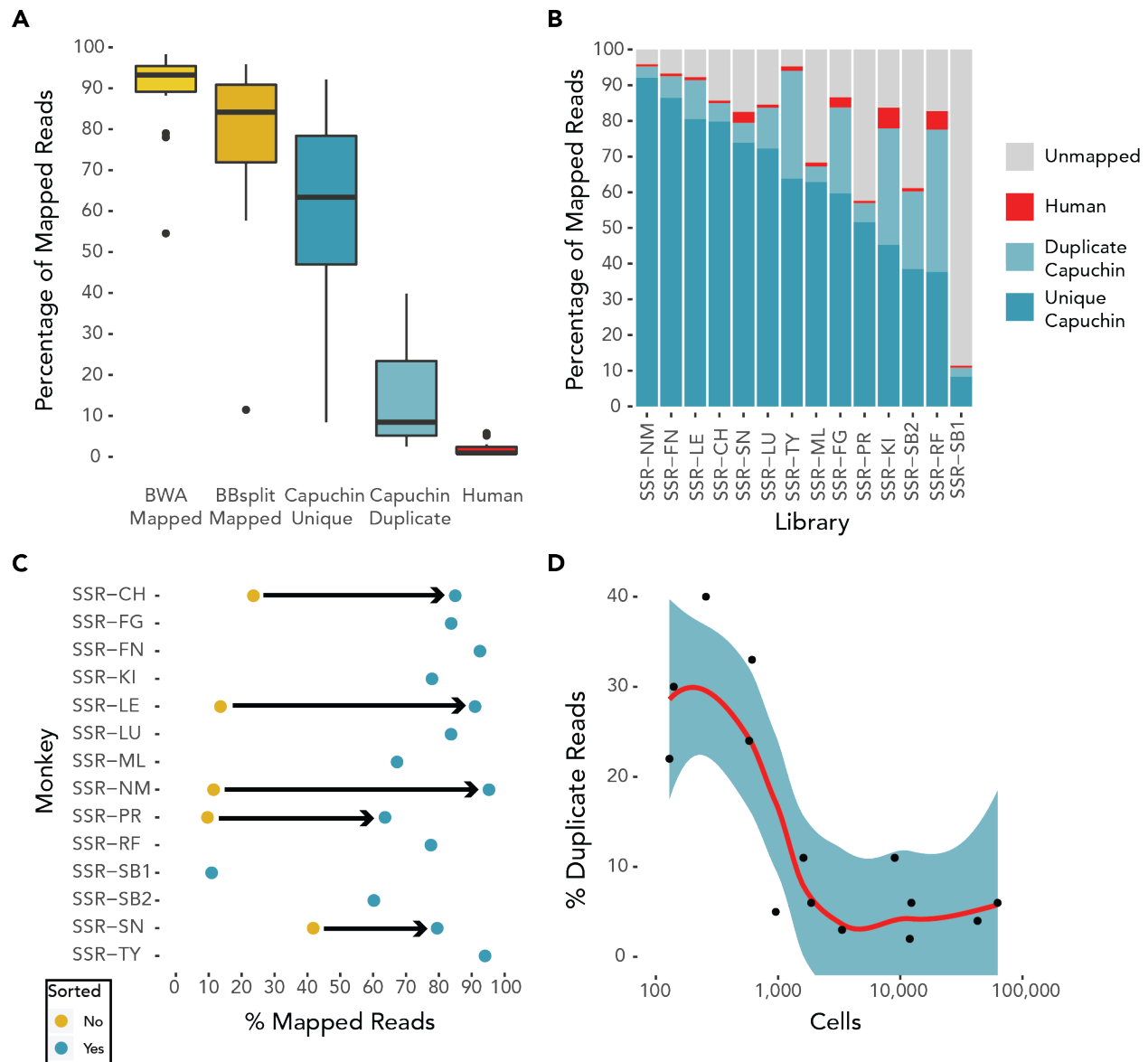
747

748 **FIGURES**  
749



750  
751  
752  
753  
754  
755  
756  
757  
758

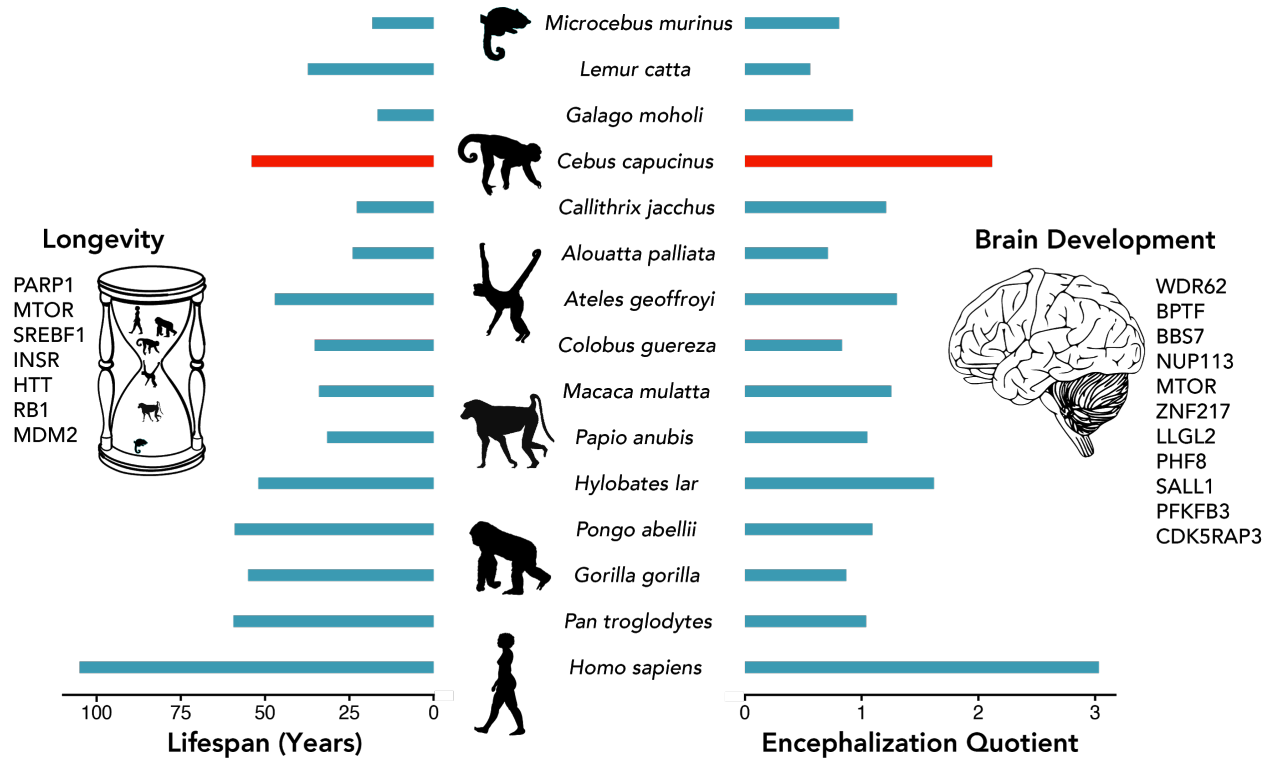
**Figure 1:** Sector Santa Rosa (SSR) during wet (left) and dry (middle) seasons. Right: Map of sampling locations in Costa Rica. The two northern sites, SSR and Cañas, have tropical dry forest biomes, whereas the two southern sites, Quepos and Manuel Antonio are tropical wet forests. Photos - Amanda Melin; Drawing of white faced capuchin monkey - Alejandra Tejada-Martinez; Map: Eric Gaba – Wikimedia Commons user: Sting



759  
760

761 **Figure 2:** Mapping percentages of sequencing reads from RNAlater preserved fDNA libraries  
762 prepared with FACS for A) all samples [Box-plot elements: center line, median; box limits, upper  
763 and lower quartiles; whiskers, 1.5x interquartile range; points, outliers], and B) individual  
764 libraries. C) Increase in mapping rate for RNAlater preserved samples. D) Relationship between  
765 mapped read duplication and number of cells with LOESS smoothing. The duplicate rate  
766 decreases sharply once a threshold of about 1,000 cells is reached.

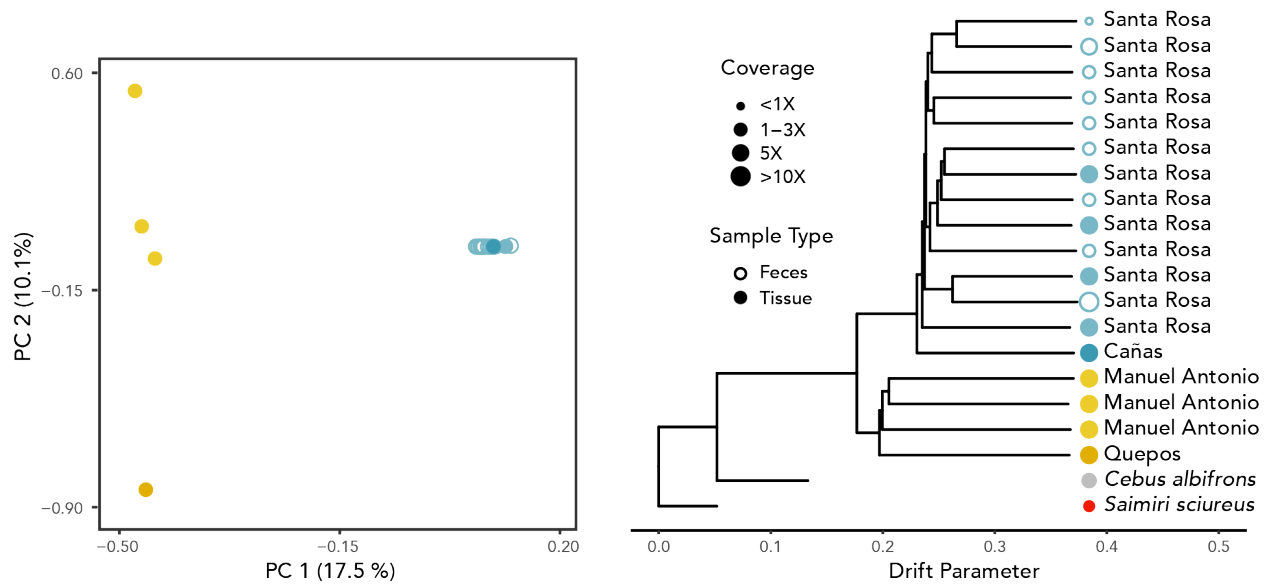
767  
768



769  
770  
771  
772  
773  
774

**Figure 3:** Genes under positive selection in white-faced capuchin monkeys that are associated with longevity and brain development. Values from *Cebus capucinus* are used in place of *Cebus imitator*, given the recent taxonomic split.

775



776

Population/Species: ● Santa Rosa ● Cañas ● Manuel Antonio ● Quepos ● Cebus albifrons ● Saimiri sciureus

777

778

779

780

781

782

783

784

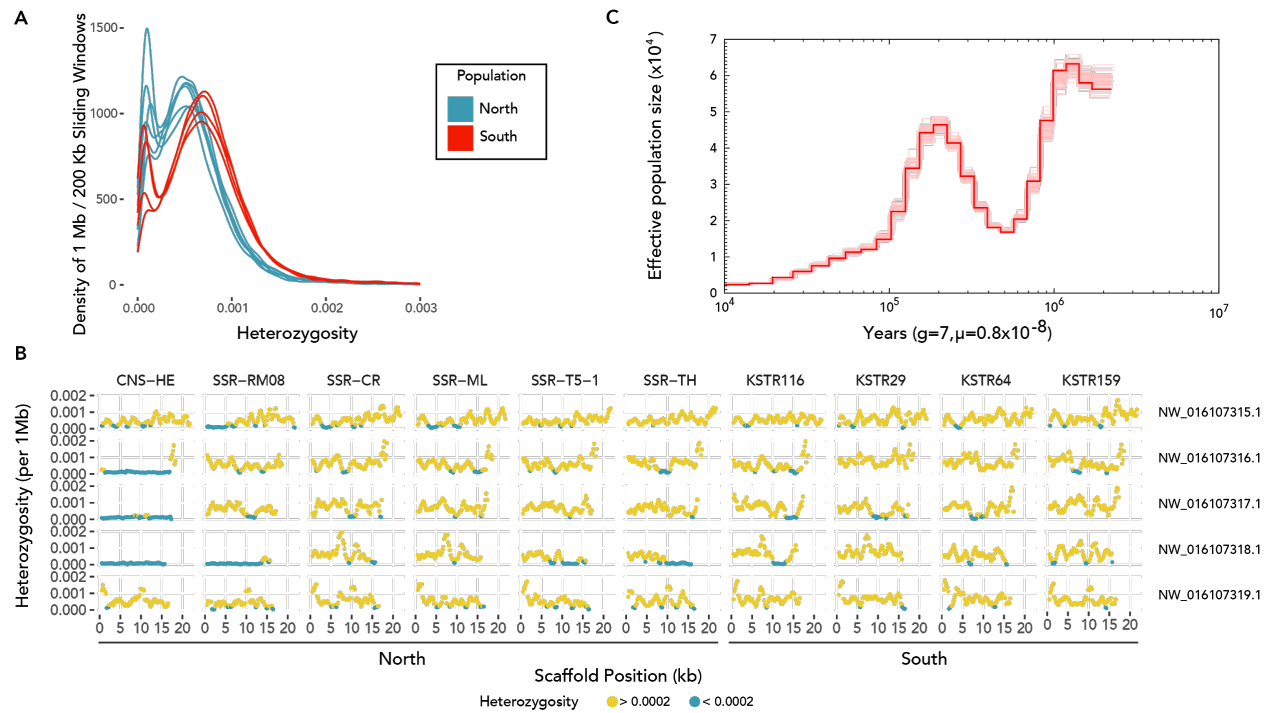
785

786

787

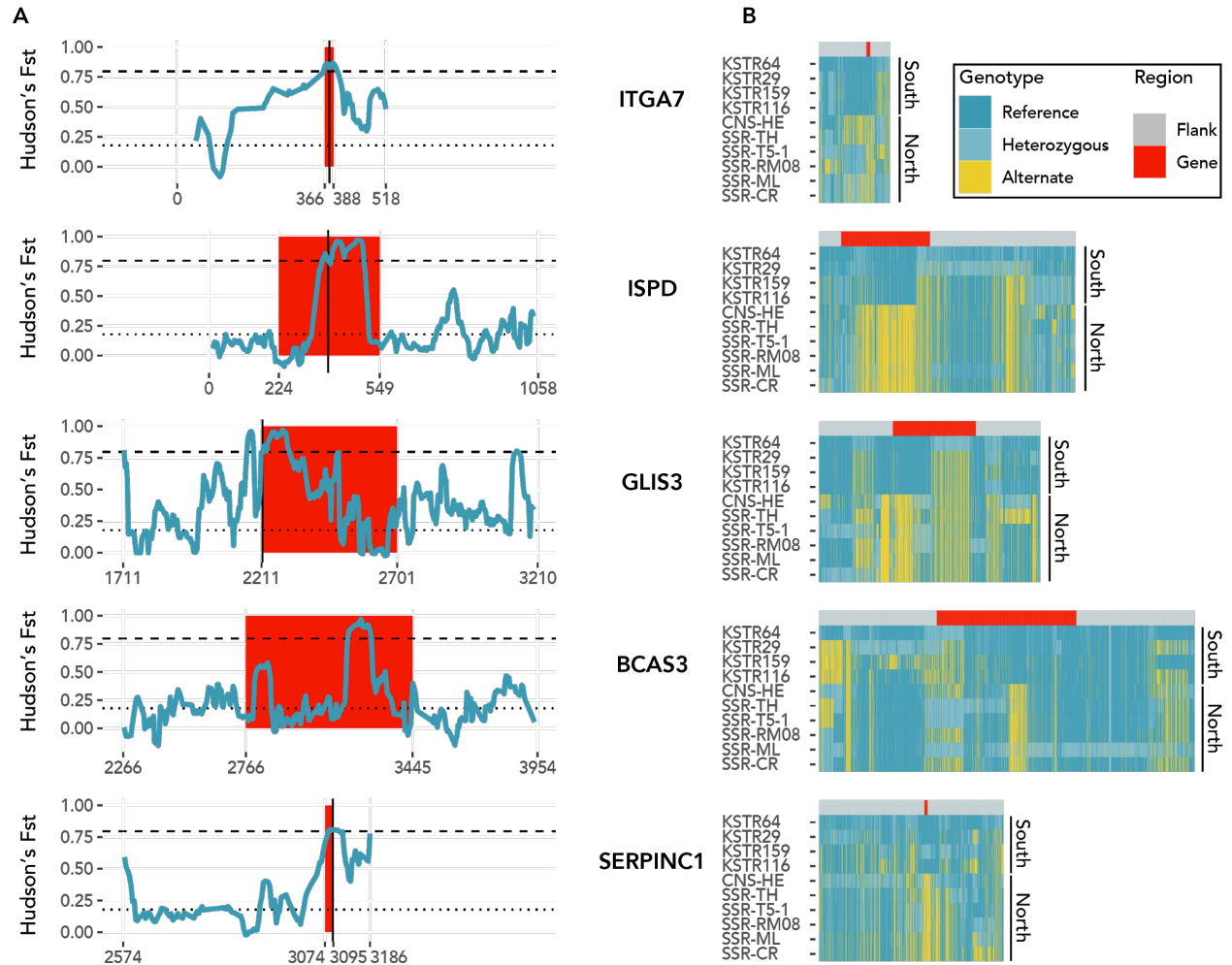
**Figure 4:** Population subdivision in *Cebus imitator*. Left: Principal components of 13 fecal and 10 blood/tissue libraries from white faced capuchins. Individuals from northern and southern sites separate on PC 1. Low- and high-coverage *C. imitator* samples from Santa Rosa plot in the same cluster. Right: Maximum likelihood tree of 9 fecal and 10 blood/tissue libraries from *C. imitator* (samples with less than 0.5X coverage were excluded). Among the white-faced capuchin samples, individuals from northern (dry forest) and southern (wet forest) regions form the primary split; secondary splits reflect the individuals from different sites within regions. The short branch lengths of the outgroups are a result of only polymorphic positions within *C. imitator* being used to construct the tree.





788  
789  
790  
791  
792  
793  
794  
795  
796

**Figure 5:** A: Density plot of 1 Mb windows with a slide of 200 Kb in northern and southern populations. The distribution of windows from the northern population indicates lower heterozygosity than the southern distribution. The individuals from the southern population show consistently higher values. B: Long runs of homozygosity in the 5 largest scaffolds. Blue dots represent windows with depleted heterozygosity. The individuals with the longest runs of homozygosity come from the northern population. C: PSMC plot of effective population size over time.



797

798

799 **Figure 6:** Highly differentiated genes between wet and dry forest populations involved in

800 diabetes, kidney function, and creatinine levels. A: Hudson's  $F_{ST}$  within windows of 20kb with a

801 4 kb slide. Gene regions are in red, flanked by 500 kb (or length to beginning or end of scaffold)

802 of sequence. X-axis values correspond to position along the scaffold. The dotted line indicates

803 average  $F_{ST}$  value across all windows ( $F_{ST} = 0.178$ ), and the dashed line represents the top

804 0.5% of values ( $F_{ST} = 0.797$ ). Vertical black lines indicate a non-synonymous SNP with an

805  $F_{st} \geq 0.750$ , excluding BCAS3 (see Results). B: Heatmaps indicating the pattern of SNP

806 variation within and surrounding highly divergent genes. SNVs within the genes are located

806 under the red band and those within 200 kb of flanking region under the gray bands.

807

808

809

810

## 811 REFERENCES

- 812 1. DeCasien AR, Williams SA, Higham JP. Primate brain size is predicted by diet but not  
813 sociality. *Nature Ecology & Evolution*. Macmillan Publishers Limited, part of Springer  
814 Nature.; 2017;1:0112.
- 815 2. Street SE, Navarrete AF, Reader SM, Laland KN. Coevolution of cultural intelligence,  
816 extended life history, sociality, and brain size in primates. *Proc Natl Acad Sci U S A*.  
817 2017;114:7908–14.
- 818 3. Aiello LC, Wheeler PE. The expensive-tissue hypothesis. *Curr Anthropol*. 1995;36:199–221.
- 819 4. Washburn SL. Tools and human evolution. *Sci Am*. 1960;203:63–75.
- 820 5. Kaplan H, Hill K, Lancaster J, Magdalena Hurtado A. A theory of human life history evolution:  
821 Diet, intelligence, and longevity [Internet]. *Evolutionary Anthropology: Issues, News, and*  
822 *Reviews*. 2000. p. 156–85.
- 823 6. Russon AE, Begun DR. Evolutionary origins of great ape intelligence: an integrated view  
824 [Internet]. *The Evolution of Thought*. 2004. p. 353–68. Available from:  
825 <http://dx.doi.org/10.1017/cbo9780511542299.023>
- 826 7. Melin AD, Young HC, Mosdossy KN, Fedigan LM. Seasonality, extractive foraging and the  
827 evolution of primate sensorimotor intelligence. *J Hum Evol*. 2014;71:77–86.
- 828 8. Fragaszy DM, Visalberghi E, Fedigan LM. *The Complete Capuchin: The Biology of the Genus*  
829 *Cebus*. Cambridge University Press; 2004.
- 830 9. De Petrillo F, Rosati AG. Ecological rationality: Convergent decision-making in apes and  
831 capuchins. *Behav Processes*. 2019;164:201–13.
- 832 10. Barrett BJ, Monteza-Moreno CM, Dogandžić T, Zwyns N, Ibáñez A, Crofoot MC. Habitual  
833 stone-tool-aided extractive foraging in white-faced capuchins, *Cebus capucinus*. *R Soc open*  
834 *sci*. 2018;5:181002.
- 835 11. Emery NJ. Are Corvids “Feathered Apes”? Cognitive evolution in crows, jays, rooks and  
836 jackdaws. In: Watanabe S, editor. *Comparative Analysis of Minds*. Keio University Press:  
837 Tokyo.; 2004. p. 181–213.
- 838 12. Marino L. Convergence of complex cognitive abilities in cetaceans and primates. *Brain*  
839 *Behav Evol*. 2002;59:21–32.
- 840 13. Lynch Alfaro JW, Boubli JP, Olson LE, Di Fiore A, Wilson B, Gutiérrez-Espeleta GA, et al.  
841 Explosive Pleistocene range expansion leads to widespread Amazonian sympatry between  
842 robust and gracile capuchin monkeys: Biogeography of Neotropical capuchin monkeys. *J*  
843 *Biogeogr*. 2012;39:272–88.
- 844 14. Boubli JP, Rylands AB, Farias IP, Alfaro ME, Alfaro JL. *Cebus* phylogenetic relationships: a  
845 preliminary reassessment of the diversity of the untufted capuchin monkeys. *Am J Primatol*.  
846 2012;74:381–93.

- 847 15. Johnson SE, Brown KA. The Specialist Capuchin? Using Ecological Niche Models to  
848 Compare Niche Breadth in Mesoamerican Primates. In: Kalbitzer U, Jack KM, editors. Primate  
849 Life Histories, Sex Roles, and Adaptability: Essays in Honour of Linda M Fedigan. Cham:  
850 Springer International Publishing; 2018. p. 311–29.
- 851 16. Kuehn M, Welsch H, Zahnert T, Hummel T. Changes of pressure and humidity affect  
852 olfactory function. *Eur Arch Otorhinolaryngol*. 2008;265:299–302.
- 853 17. Benignus VA, Prah JD. Flow thresholds of nonodorous air through the human naris as a  
854 function of temperature and humidity. *Percept Psychophys*. 1980;27:569–73.
- 855 18. Mollon JD. “Tho’she kneel’d in that place where they grew...” The uses and origins of  
856 primate colour vision. *J Exp Biol* [Internet]. [jeb.biologists.org](http://jeb.biologists.org); 1989; Available from:  
857 <https://jeb.biologists.org/content/146/1/21.short>
- 858 19. Campos FA, Fedigan LM. Behavioral adaptations to heat stress and water scarcity in white-  
859 faced capuchins (*Cebus capucinus*) in Santa Rosa National Park, Costa Rica. *Am J Phys*  
860 *Anthropol*. Wiley Online Library; 2009;138:101–11.
- 861 20. Mosdossy KN, Melin AD, Fedigan LM. Quantifying seasonal fallback on invertebrates, pith,  
862 and bromeliad leaves by white-faced capuchin monkeys (*Cebus capucinus*) in a tropical dry  
863 forest. *Am J Phys Anthropol*. 2015;158:67–77.
- 864 21. Proffitt T, Luncz LV, Falótico T, Ottoni EB, de la Torre I, Haslam M. Wild monkeys flake  
865 stone tools. *Nature*. 2016;539:85–8.
- 866 22. Izar P, Verderane MP, Peternelli-Dos-Santos L, Mendonça-Furtado O, Presotto A, Tokuda  
867 M, et al. Flexible and conservative features of social systems in tufted capuchin monkeys:  
868 comparing the socioecology of *Sapajus libidinosus* and *Sapajus nigritus*. *Am J Primatol*.  
869 2012;74:315–31.
- 870 23. Merkt JR, Taylor CR. “Metabolic switch” for desert survival [Internet]. *Proceedings of the*  
871 *National Academy of Sciences*. 1994. p. 12313–6. Available from:  
872 <http://dx.doi.org/10.1073/pnas.91.25.12313>
- 873 24. Pontzer H, Raichlen DA, Shumaker RW, Ocobock C, Wich SA. Metabolic adaptation for low  
874 energy throughput in orangutans. *Proc Natl Acad Sci U S A*. 2010;107:14048–52.
- 875 25. Schmidt-Nielsen K, Schmidt-Nielsen B. Water metabolism of desert mammals 1. *Physiol*  
876 *Rev*. 1952;32:135–66.
- 877 26. Cain JW III, Krausman PR, Rosenstock SS, Turner JC. Mechanisms of Thermoregulation  
878 and Water Balance in Desert Ungulates. *Wildl Soc Bull*. Wiley Online Library; 2006;34:570–81.
- 879 27. Olender T, Waszak SM, Viavant M, Khen M, Ben-Asher E, Reyes A, et al. Personal receptor  
880 repertoires: olfaction as a model. *BMC Genomics*. 2012;13:414.
- 881 28. Jacobs RL, MacFie TS, Spriggs AN, Baden AL, Morelli TL, Irwin MT, et al. Novel opsin gene  
882 variation in large-bodied, diurnal lemurs. *Biol Lett* [Internet]. 2017;13. Available from:  
883 <http://dx.doi.org/10.1098/rsbl.2017.0050>

- 884 29. Lachance J, Vernot B, Elbers CC, Ferwerda B, Froment A, Bodo J-M, et al. Evolutionary  
885 history and adaptation from high-coverage whole-genome sequences of diverse African hunter-  
886 gatherers. *Cell*. 2012;150:457–69.
- 887 30. Morgulis A, Gertz EM, Schäffer AA, Agarwala R. WindowMasker: window-based masker for  
888 sequenced genomes. *Bioinformatics*. 2006;22:134–41.
- 889 31. Rice ES, Green RE. New Approaches for Genome Assembly and Scaffolding. *Annu Rev*  
890 *Anim Biosci*. 2019;7:17–40.
- 891 32. Yang Z. PAML 4: phylogenetic analysis by maximum likelihood. *Mol Biol Evol*.  
892 2007;24:1586–91.
- 893 33. Huang DW, Sherman BT, Lempicki RA. Systematic and integrative analysis of large gene  
894 lists using DAVID bioinformatics resources [Internet]. *Nature Protocols*. 2009. p. 44–57.  
895 Available from: <http://dx.doi.org/10.1038/nprot.2008.211>
- 896 34. Memon MM, Raza SI, Basit S, Kousar R, Ahmad W, Ansar M. A novel WDR62 mutation  
897 causes primary microcephaly in a Pakistani family. *Mol Biol Rep*. 2013;40:591–5.
- 898 35. Stankiewicz P, Khan TN, Szafranski P, Slattery L, Streff H, Vetrini F, et al.  
899 Haploinsufficiency of the Chromatin Remodeler BPTF Causes Syndromic Developmental and  
900 Speech Delay, Postnatal Microcephaly, and Dysmorphic Features. *Am J Hum Genet*.  
901 2017;101:503–15.
- 902 36. Guo J, Higginbotham H, Li J, Nichols J, Hirt J, Ghukasyan V, et al. Developmental  
903 disruptions underlying brain abnormalities in ciliopathies. *Nat Commun*. 2015;6:7857.
- 904 37. Fujita A, Tsukaguchi H, Koshimizu E, Nakazato H, Itoh K, Kuraoka S, et al. Homozygous  
905 splicing mutation in NUP133 causes Galloway-Mowat syndrome [Internet]. *Annals of*  
906 *Neurology*. 2018. p. 814–28. Available from: <http://dx.doi.org/10.1002/ana.25370>
- 907 38. Crino PB. mTOR signaling in epilepsy: insights from malformations of cortical development.  
908 *Cold Spring Harb Perspect Med* [Internet]. 2015;5. Available from:  
909 <http://dx.doi.org/10.1101/cshperspect.a022442>
- 910 39. Bertipaglia C, Gonçalves JC, Vallee RB. Nuclear migration in mammalian brain  
911 development. *Semin Cell Dev Biol*. 2018;82:57–66.
- 912 40. Laumonier F, Holbert S, Ronce N, Faravelli F, Lenzner S, Schwartz CE, et al. Mutations in  
913 PHF8 are associated with X linked mental retardation and cleft lip/cleft palate. *J Med Genet*.  
914 2005;42:780–6.
- 915 41. Li Y, de Magalhães JP. Accelerated protein evolution analysis reveals genes and pathways  
916 associated with the evolution of mammalian longevity. *Age*. 2013;35:301–14.
- 917 42. Tacutu R, Thornton D, Johnson E, Budovsky A, Barardo D, Craig T, et al. Human Ageing  
918 Genomic Resources: new and updated databases. *Nucleic Acids Res*. 2018;46:D1083–90.
- 919 43. Grube K, Bürkle A. Poly(ADP-ribose) polymerase activity in mononuclear leukocytes of 13  
920 mammalian species correlates with species-specific life span. *Proc Natl Acad Sci U S A*.

- 921 1992;89:11759–63.
- 922 44. Cornu M, Albert V, Hall MN. mTOR in aging, metabolism, and cancer. *Curr Opin Genet Dev.*  
923 2013;23:53–62.
- 924 45. de Magalhães JP, Stevens M, Thornton D. The Business of Anti-Aging Science. *Trends*  
925 *Biotechnol.* 2017;35:1062–73.
- 926 46. Fujii N, Narita T, Okita N, Kobayashi M, Furuta Y, Chujo Y, et al. Sterol regulatory element-  
927 binding protein-1c orchestrates metabolic remodeling of white adipose tissue by caloric  
928 restriction. *Aging Cell.* Wiley Online Library; 2017;16:508–17.
- 929 47. Plank M, Wuttke D, van Dam S, Clarke SA, de Magalhães JP. A meta-analysis of caloric  
930 restriction gene expression profiles to infer common signatures and regulatory mechanisms. *Mol*  
931 *Biosyst.* 2012;8:1339–49.
- 932 48. Kenyon CJ. The genetics of ageing. *Nature.* 2010;464:504–12.
- 933 49. Zheng S, Clabough EBD, Sarkar S, Futter M, Rubinsztein DC, Zeitlin SO. Deletion of the  
934 huntingtin polyglutamine stretch enhances neuronal autophagy and longevity in mice. *PLoS*  
935 *Genet.* 2010;6:e1000838.
- 936 50. Long H, Huang K. Transport of Ciliary Membrane Proteins. *Front Cell Dev Biol.* 2020;7:381.
- 937 51. Lu Z, Wang F, Liang M. SerpinC1/Antithrombin III in kidney-related diseases. *Clin Sci.*  
938 2017;131:823–31.
- 939 52. Kauffmann RH, Veltkamp JJ, Van Tilburg NH, Van Es LA. Acquired antithrombin III  
940 deficiency and thrombosis in the nephrotic syndrome. *Am J Med.* 1978;65:607–13.
- 941 53. Lau SO, Tkachuck JY, Hasegawa DK, Edson JR. Plasminogen and antithrombin III  
942 deficiencies in the childhood nephrotic syndrome associated with plasminogenuria and  
943 antithrombinuria. *J Pediatr.* 1980;96:390–2.
- 944 54. Citak A, Emre S, Sirin A, Bilge I, Nayır A. Hemostatic problems and thromboembolic  
945 complications in nephrotic children. *Pediatr Nephrol.* 2000;14:138–42.
- 946 55. Liang M, Lee NH, Wang H, Greene AS, Kwitek AE, Kaldunski ML, et al. Molecular networks  
947 in Dahl salt-sensitive hypertension based on transcriptome analysis of a panel of consomic rats.  
948 *Physiol Genomics.* 2008;34:54–64.
- 949 56. Tomczykowska M, Bielak J, Bodys A. Evaluation of platelet activation, plasma antithrombin  
950 III and alpha2-antiplasmin activities in hypertensive patients. *Ann Univ Mariae Curie*  
951 *Skłodowska Med.* 2003;58:15–20.
- 952 57. Morris AP, Le TH, Wu H, Akbarov A, van der Most PJ, Hemani G, et al. Trans-ethnic kidney  
953 function association study reveals putative causal genes and effects on kidney-specific disease  
954 aetiologies. *Nat Commun.* 2019;10:29.
- 955 58. Okada Y, Sim X, Go MJ, Wu J-Y, Gu D, Takeuchi F, et al. Meta-analysis identifies multiple  
956 loci associated with kidney function-related traits in east Asian populations. *Nat Genet.*

- 957 2012;44:904–9.
- 958 59. Bergstrom ML, Emery Thompson M, Melin AD, Fedigan LM. Using urinary parameters to  
959 estimate seasonal variation in the physical condition of female white-faced capuchin monkeys  
960 (*Cebus capucinus imitator*). *Am J Phys Anthropol* [Internet]. 2017; Available from:  
961 <http://dx.doi.org/10.1002/ajpa.23239>
- 962 60. Myers VC, Fine MS. The creatine content of muscle under normal conditions. Its relation to  
963 the urinary creatinine. *Proc Soc Exp Biol Med*. SAGE Publications; 1912;10:10–1.
- 964 61. Cirak S, Foley AR, Herrmann R, Willer T, Yau S, Stevens E, et al. ISPD gene mutations are  
965 a common cause of congenital and limb-girdle muscular dystrophies. *Brain*. 2013;136:269–81.
- 966 62. Roscioli T, Kamsteeg E-J, Buysse K, Maystadt I, van Reeuwijk J, van den Elzen C, et al.  
967 Mutations in ISPD cause Walker-Warburg syndrome and defective glycosylation of  $\alpha$ -  
968 dystroglycan. *Nat Genet*. Nature Publishing Group; 2012;44:581–5.
- 969 63. Mayer U, Saher G, Fässler R, Bornemann A, Echtermeyer F, von der Mark H, et al.  
970 Absence of integrin alpha 7 causes a novel form of muscular dystrophy. *Nat Genet*.  
971 1997;17:318–23.
- 972 64. Zhang Q, Bethmann C, Worth NF, Davies JD, Wasner C, Feuer A, et al. Nesprin-1 and -2  
973 are involved in the pathogenesis of Emery Dreifuss muscular dystrophy and are critical for  
974 nuclear envelope integrity. *Hum Mol Genet*. 2007;16:2816–33.
- 975 65. Doe JA, Wuebbles RD, Allred ET, Rooney JE, Elorza M, Burkin DJ. Transgenic  
976 overexpression of the  $\alpha 7$  integrin reduces muscle pathology and improves viability in the dy(W)  
977 mouse model of merosin-deficient congenital muscular dystrophy type 1A. *J Cell Sci*.  
978 2011;124:2287–97.
- 979 66. Amin S, Cook B, Zhou T, Ghazizadeh Z, Lis R, Zhang T, et al. Discovery of a drug  
980 candidate for GLIS3-associated diabetes. *Nat Commun*. 2018;9:2681.
- 981 67. Melin AD, Fedigan LM, Hiramatsu C, Kawamura S. Polymorphic color vision in white-faced  
982 capuchins (*Cebus capucinus*): Is there foraging niche divergence among phenotypes? *Behav*  
983 *Ecol Sociobiol*. 2007;62:659–70.
- 984 68. Hiramatsu C, Tsutsui T, Matsumoto Y, Aureli F, Fedigan LM, Kawamura S. Color-vision  
985 polymorphism in wild capuchins (*Cebus capucinus*) and spider monkeys (*Ateles geoffroyi*) in  
986 Costa Rica. *Am J Primatol*. 2005;67:447–61.
- 987 69. Kennedy BG, Haley BE, Mangini NJ. Creatine kinase in human retinal pigment epithelium.  
988 *Exp Eye Res*. 2000;70:183–90.
- 989 70. Gerding WM, Schreiber S, Schulte-Middelmann T, de Castro Marques A, Atorf J, Akkad DA,  
990 et al. *Ccdc66* null mutation causes retinal degeneration and dysfunction. *Hum Mol Genet*.  
991 2011;20:3620–31.
- 992 71. Schreiber S, Petrasch-Parwez E, Porrmann-Kelterbaum E, Förster E, Epplen JT, Gerding  
993 WM. Neurodegeneration in the olfactory bulb and olfactory deficits in the *Ccdc66* *-/-* mouse  
994 model for retinal degeneration. *IBRO Reports*. Elsevier; 2018;5:43–53.

- 995 72. Tsutsui K, Otoh M, Sakurai K, Suzuki-Hashido N, Hayakawa T, Misaka T, et al. Variation in  
996 ligand responses of the bitter taste receptors TAS2R1 and TAS2R4 among New World  
997 monkeys. *BMC Evol Biol.* 2016;16:208.
- 998 73. Roth G, Dicke U. Evolution of the brain and intelligence. *Trends Cogn Sci.* 2005;9:250–7.
- 999 74. Gibson KR. Evolution of human intelligence: the roles of brain size and mental construction.  
1000 *Brain Behav Evol.* 2002;59:10–20.
- 1001 75. Reader SM, Laland KN. Social intelligence, innovation, and enhanced brain size in primates.  
1002 *Proc Natl Acad Sci U S A.* 2002;99:4436–41.
- 1003 76. Muntané G, Farré X, Rodríguez JA, Pegueroles C, Hughes DA, de Magalhães JP, et al.  
1004 Biological Processes Modulating Longevity across Primates: A Phylogenetic Genome-Phenome  
1005 Analysis. *Mol Biol Evol.* 2018;35:1990–2004.
- 1006 77. Freitas AA, de Magalhães JP. A review and appraisal of the DNA damage theory of ageing.  
1007 *Mutat Res.* 2011;728:12–22.
- 1008 78. Zhang G, Cowled C, Shi Z, Huang Z, Bishop-Lilly KA, Fang X, et al. Comparative analysis of  
1009 bat genomes provides insight into the evolution of flight and immunity. *Science.* 2013;339:456–  
1010 60.
- 1011 79. Keane M, Semeiks J, Webb AE, Li YI, Quesada V, Craig T, et al. Insights into the evolution  
1012 of longevity from the bowhead whale genome. *Cell Rep.* 2015;10:112–22.
- 1013 80. Seim I, Fang X, Xiong Z, Lobanov AV, Huang Z, Ma S, et al. Genome analysis reveals  
1014 insights into physiology and longevity of the Brandt’s bat *Myotis brandtii*. *Nat Commun.*  
1015 2013;4:2212.
- 1016 81. Valenzano DR, Benayoun BA, Singh PP, Zhang E, Etter PD, Hu C-K, et al. The African  
1017 Turquoise Killifish Genome Provides Insights into Evolution and Genetic Architecture of  
1018 Lifespan. *Cell.* 2015;163:1539–54.
- 1019 82. de Magalhães JP, Costa J, Church GM. An analysis of the relationship between  
1020 metabolism, developmental schedules, and longevity using phylogenetic independent contrasts.  
1021 *J Gerontol A Biol Sci Med Sci.* 2007;62:149–60.
- 1022 83. Orkin JD, Campos FA, Myers MS, Cheves Hernandez SE, Guadamuz A, Melin AD.  
1023 Seasonality of the gut microbiota of free-ranging white-faced capuchins in a tropical dry forest.  
1024 *ISME J.* 2019;13:183–96.
- 1025 84. Mallott EK, Amato KR. The microbial reproductive ecology of white-faced capuchins (*Cebus*  
1026 *capucinus*). *Am J Primatol.* 2018;e22896.
- 1027 85. Young RA. Fat, Energy and Mammalian Survival. *Integr Comp Biol.* Narnia; 1976;16:699–  
1028 710.
- 1029 86. Niimura Y, Matsui A, Touhara K. Acceleration of Olfactory Receptor Gene Loss in Primate  
1030 Evolution: Possible Link to Anatomical Change in Sensory Systems and Dietary Transition. *Mol*  
1031 *Biol Evol.* 2018;35:1437–50.



- 1032 87. Go Y. Lineage-specific expansions and contractions of the bitter taste receptor gene  
1033 repertoire in vertebrates. *Mol Biol Evol.* 2006;23:964–72.
- 1034 88. Li D, Zhang J. Diet shapes the evolution of the vertebrate bitter taste receptor gene  
1035 repertoire. *Mol Biol Evol.* 2014;31:303–9.
- 1036 89. Yoder AD, Larsen PA. The molecular evolutionary dynamics of the vomeronasal receptor  
1037 (class 1) genes in primates: a gene family on the verge of a functional breakdown. *Front*  
1038 *Neuroanat.* 2014;8:153.
- 1039 90. Moriya-Ito K, Hayakawa T, Suzuki H, Hagino-Yamagishi K, Nikaido M. Evolution of  
1040 vomeronasal receptor 1 (V1R) genes in the common marmoset (*Callithrix jacchus*). *Gene.*  
1041 2018;642:343–53.
- 1042 91. Alfaro JW, Lynch Alfaro JW, de Sousa E Silva J, Rylands AB. How Different Are Robust  
1043 and Gracile Capuchin Monkeys? An Argument for the Use of *Sapajus* and *Cebus*. *Am J*  
1044 *Primatol.* 2012;74:273–86.
- 1045 92. Janzen D. Tropical dry forest: area de Conservación Guanacaste, northwestern Costa Rica.  
1046 In: Perrow M DA, editor. *Handbook of Ecological Restoration: Restoration in Practice.*  
1047 Cambridge University Press, Cambridge; 2002. p. 559–83.
- 1048 93. Campos FA. A synthesis of long-term environmental change in Santa Rosa. In: Kalbitzer U,  
1049 Jack KM, editors. *Primate Life Histories, Sex Roles, and Adaptability - Essays in Honour of*  
1050 *Linda M Fedigan.* Springer, New York; 2018.
- 1051 94. Fedigan L, Rose-Wiles L. See how they grow: Tracking capuchin monkey populations in a  
1052 regenerating Costa Rican dry forest. In: Norconk MA, Rosenberger AL, Garber PA, editors.  
1053 *Adaptive radiations of Neotropical primates.* Springer; 1996. p. 289–307.
- 1054 95. Rinke C, Lee J, Nath N, Goudeau D, Thompson B, Poulton N, et al. Obtaining genomes  
1055 from uncultivated environmental microorganisms using FACS-based single-cell genomics. *Nat*  
1056 *Protoc.* 2014;9:1038–48.
- 1057 96. Gnerre S, Maccallum I, Przybylski D, Ribeiro FJ, Burton JN, Walker BJ, et al. High-quality  
1058 draft assemblies of mammalian genomes from massively parallel sequence data. *Proc Natl*  
1059 *Acad Sci U S A.* 2011;108:1513–8.
- 1060 97. Fu L, Niu B, Zhu Z, Wu S, Li W. CD-HIT: accelerated for clustering the next-generation  
1061 sequencing data. *Bioinformatics.* 2012;28:3150–2.
- 1062 98. Altenhoff AM, Levy J, Zarowiecki M, Tomiczek B, Warwick Vesztrocy A, Dalquen DA, et al.  
1063 OMA standalone: orthology inference among public and custom genomes and transcriptomes.  
1064 *Genome Res.* 2019;29:1152–63.
- 1065 99. Brown JW, Walker JF, Smith SA. Phyx: phylogenetic tools for unix. *Bioinformatics.*  
1066 2017;33:1886–8.
- 1067 100. Katoh K, Standley DM. MAFFT multiple sequence alignment software version 7:  
1068 improvements in performance and usability. *Mol Biol Evol.* 2013;30:772–80.

- 1069 101. Hubisz MJ, Pollard KS, Siepel A. PHAST and RPHAST: phylogenetic analysis with  
1070 space/time models. *Brief Bioinform.* 2011;12:41–51.
- 1071 102. Huerta-Cepas J, Serra F, Bork P. ETE 3: Reconstruction, Analysis, and Visualization of  
1072 Phylogenomic Data. *Mol Biol Evol.* 2016;33:1635–8.
- 1073 103. Zhang J. Evaluation of an Improved Branch-Site Likelihood Method for Detecting Positive  
1074 Selection at the Molecular Level [Internet]. *Molecular Biology and Evolution.* 2005. p. 2472–9.  
1075 Available from: <http://dx.doi.org/10.1093/molbev/msi237>
- 1076 104. Bolger AM, Lohse M, Usadel B. Trimmomatic: a flexible trimmer for Illumina sequence  
1077 data. *Bioinformatics.* 2014;30:2114–20.
- 1078 105. Li H, Durbin R. Fast and accurate short read alignment with Burrows-Wheeler transform.  
1079 *Bioinformatics.* 2009;25:1754–60.
- 1080 106. Li H, Handsaker B, Wysoker A, Fennell T, Ruan J, Homer N, et al. The Sequence  
1081 Alignment/Map format and SAMtools. *Bioinformatics.* 2009;25:2078–9.
- 1082 107. McKenna A, Hanna M, Banks E, Sivachenko A, Cibulskis K, Kernytsky A, et al. The  
1083 Genome Analysis Toolkit: a MapReduce framework for analyzing next-generation DNA  
1084 sequencing data. *Genome Res.* 2010;20:1297–303.
- 1085 108. Bushnell B. BBMap short read aligner. University of California, Berkeley, California URL  
1086 <http://sourceforge.net/projects/bbmap>. 2016;
- 1087 109. Price AL, Patterson NJ, Plenge RM, Weinblatt ME, Shadick NA, Reich D. Principal  
1088 components analysis corrects for stratification in genome-wide association studies. *Nat Genet.*  
1089 2006;38:904–9.
- 1090 110. Pickrell JK, Pritchard JK. Inference of population splits and mixtures from genome-wide  
1091 allele frequency data. *PLoS Genet.* 2012;8:e1002967.
- 1092 111. Li H, Durbin R. Inference of human population history from individual whole-genome  
1093 sequences. *Nature.* 2011;475:493–6.
- 1094 112. Monroy Kuhn JM, Jakobsson M, Günther T. Estimating genetic kin relationships in  
1095 prehistoric populations. *PLoS One.* 2018;13:e0195491.
- 1096 113. Quinlan AR, Hall IM. BEDTools: a flexible suite of utilities for comparing genomic features.  
1097 *Bioinformatics.* 2010;26:841–2.
- 1098 114. Bhatia G, Patterson N, Sankararaman S, Price AL. Estimating and interpreting F<sub>ST</sub>: the  
1099 impact of rare variants. *Genome Res.* 2013;23:1514–21.
- 1100 115. Chen J, Bardes EE, Aronow BJ, Jegga AG. ToppGene Suite for gene list enrichment  
1101 analysis and candidate gene prioritization. *Nucleic Acids Res.* 2009;37:W305–11.
- 1102 116. Niimura Y, Nei M. Extensive gains and losses of olfactory receptor genes in mammalian  
1103 evolution. *PLoS One.* [journals.plos.org](http://journals.plos.org); 2007;2:e708.
- 1104 117. Li H. A statistical framework for SNP calling, mutation discovery, association mapping and

- 1105 population genetical parameter estimation from sequencing data. *Bioinformatics*. 2011;27:2987–  
1106 93.
- 1107 118. Hayden S, Bekaert M, Crider TA, Mariani S, Murphy WJ, Teeling EC. Ecological adaptation  
1108 determines functional mammalian olfactory subgenomes. *Genome Res*. 2010;20:1–9.
- 1109 119. Hayden S, Bekaert M, Goodbla A, Murphy WJ, Dávalos LM, Teeling EC. A cluster of  
1110 olfactory receptor genes linked to frugivory in bats. *Mol Biol Evol*. 2014;31:917–27.
- 1111 120. Danecek P, Auton A, Abecasis G, Albers CA, Banks E, De Pisto MA, et al. The variant call  
1112 format and VCFtools. *BIOINFORMATICS APPLICATIONS NOTE* [Internet]. 2011;27. Available  
1113 from: <http://dx.doi.org/10.1093/bioinformatics/btr330>